Molecular Cell
Article

Centromere Identity Maintained by Nucleosomes Assembled with Histone H3 Containing the CENP-A Targeting Domain

Ben E. Black,[1,2,3,4,*] Lars E.T. Jansen,[1,2,3] Paul S. Maddox,[1,2] Daniel R. Foltz,[1,2] Arshad B. Desai,[1,2] Jagesh V. Shah,[1,2,5] and Don W. Cleveland[1,2,*]
[1] Ludwig Institute for Cancer Research
[2] Department of Cellular and Molecular Medicine
University of California, San Diego, La Jolla, CA 92093, USA
[3] These authors contributed equally to this work.
[4] Present address: Department of Biochemistry and Biophysics, University of Pennsylvania, Philadelphia, PA 19104, USA.
[5] Present Address: Department of Systems Biology, Harvard Medical School, Boston, MA 02115, USA.
*Correspondence: blackbe@mail.med.upenn.edu (B.E.B.), dcleveland@ucsd.edu (D.W.C.)
DOI 10.1016/j.molcel.2006.12.018

SUMMARY

Active centromeres are marked by nucleosomes assembled with CENP-A, a centromere-specific histone H3 variant. The CENP-A centromere targeting domain (CATD), comprised of loop 1 and the α2 helix within the histone fold, is sufficient to target histone H3 to centromeres and to generate the same conformational rigidity to the initial subnucleosomal heterotetramer with histone H4 as does CENP-A. We now show in human cells and in yeast that depletion of CENP-A is lethal, but recruitment of normal levels of kinetochore proteins, centromere-generated mitotic checkpoint signaling, chromosome segregation, and viability can be rescued by histone H3 carrying the CATD. These data offer direct support for centromere identity maintained by a unique nucleosome that serves to distinguish the centromere from the rest of the chromosome.

INTRODUCTION

The centromere is the locus that mediates accurate segregation of each chromosome at mitosis (Cleveland et al., 2003). A kinetochore, itself a large proteinaceous structure 0.5–1 μm in diameter (Rieder, 1982), is built upon each paired sister centromere during prophase and mediates attachment to spindle microtubules early in mitosis. Each kinetochore that remains unattached generates a diffusible signal capable of delaying the transition to anaphase (the no-turning-back mitotic step where sister chromosomes are separated). Chromosomes lacking a functional centromere are missegregated at mitosis because they cannot attach to the spindle or generate a mitotic checkpoint signal (Nasmyth, 2005). Likewise, chromosomes with multiple, independently acting centromeres would be susceptible to kinetochore/spindle-mediated breakage in mitosis. This is a critical step in breakage/fusion/bridge cycles involving sister-chromatid fusions that generate an effective "dicentric" chromosome, and these cycles provide a mechanism for gene amplification and aneuploidy, which are common features of human cancer (see Murnane and Sabatier [2004]). For most normal human centromeres, the underlying DNA is comprised of repetitive DNA, termed α satellite (Manuelidis and Wu, 1978; Willard, 1985), a subset of which houses a 17-mer consensus sequence (Masumoto et al., 1989) that serves as a binding site for the centromere component CENP-B (Earnshaw and Rothfield, 1985). Both this site ("the CENP-B box") and the CENP-B protein itself appear to be required for de novo centromere formation (a step that is necessary for efficient assembly of stable human artificial chromosomes [HACs]), indicating an important role in generating new centromeres starting with "naked" recombinant DNA (Ohzeki et al., 2002).

Although there may be a preference provided by α satellite arrays (and the associated CENP-B protein) for centromere positioning, neither is necessary nor sufficient for centromere inheritance, because there are examples of both de novo centromere formation (to compensate for the loss of the original centromere) and centromere silencing (when a chromosomal fusion generates a dicentric product) in patients with defined chromosomal rearrangements (Depinet et al., 1997; du Sart et al., 1997; Earnshaw and Migeon, 1985; Warburton et al., 1997). This "neocentromere" formation and the silencing of the extra centromere in "pseudo-dicentrics" are required in each case to produce chromosomes with only one functional centromere. Recently, two human cases described both phenomena: a centromere that had relocated within an intact chromosome 3 or chromosome 4, respectively, from the original location to a new location on the chromosome arm (Amor et al., 2004; Ventura et al., 2004). Although the mechanism underlying this relocation of the centromere within a chromosome is unknown, the remarkable finding was that this new location persists in multiple family

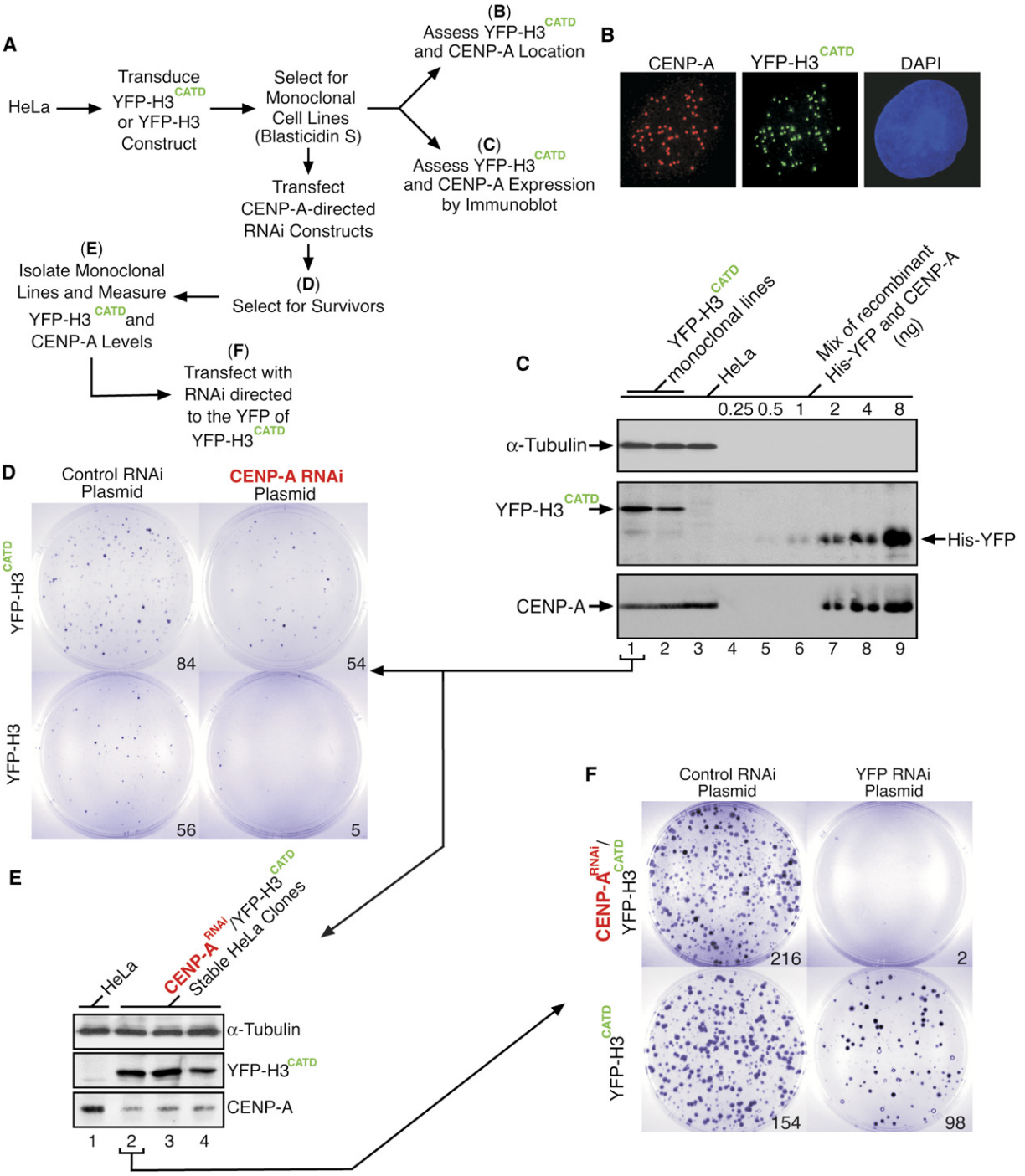

Figure 1. H3CATD Rescues the Long-Term Depletion of CENP-A by RNAi

(A) Scheme for replacing CENP-A with YFP-H3CATD.

(B) Centromere localization of endogenous CENP-A and YFP-H3CATD.

(C) Analysis of cell lines stably expressing YFP-H3CATD. 5×10^4 cells of each cell type were analyzed by immunoblot using anti-α-tubulin (top), anti-GFP (middle), or ACA (bottom). A mix of recombinant YFP and CENP-A was loaded in adjacent lanes at the indicated levels.

(D) Colony outgrowth assays in a control cell line expressing YFP-H3 and a cell line expressing H3CATD. Each line was transfected with the indicated RNAi plasmid, hygromycin selection was performed for 10 days, and colonies were fixed and stained with crystal violet.

(E) Analysis of cell lines expressing both YFP-H3CATD and CENP-A-directed RNAi. Colonies surviving CENP-A RNAi plasmid selection from YFP-H3CATD-expressing cells were isolated, expanded to cell lines, and analyzed by immunoblot.

members for at least two generations, despite the existence of an intact region within the same chromosome corresponding to the original centromere at the level of DNA sequence (megabases of repetitive α satellites that are found at the normal centromere locus, but not at these neocentromeres). The ability to permanently silence an existing centromere with no rearrangement or deletion of centromeric repeat DNA sequences, create a neocentromere at a noncentromeric region of the chromosome that lacks α satellite DNA, or both provides substantial support for the notion that human centromeres are defined epigenetically (Cleveland et al., 2003; Sullivan et al., 2001).

The most attractive candidate for an epigenetic mark for centromere function is a histone H3 variant, named centromere protein-A (CENP-A; [Earnshaw and Rothfield, 1985; Palmer and Margolis, 1985; Sullivan et al., 1994]). Together with canonical histones H2A, H2B, and H4 it forms nucleosomes at active centromeres from yeast to humans (Smith, 2002). In mitosis, this chromatin serves as the foundation for building the kinetochore (Sullivan, 2001). CENP-A is an essential protein, and its removal results in defects in kinetochore function and chromosome segregation (Goshima et al., 2003; Howman et al., 2000; Regnier et al., 2005; Stoler et al., 1995). In pseudo-dicentric chromosomes, CENP-A is absent from the inactivated centromere and is found on all known, naturally occurring neocentromeres lacking α satellite repeats (Amor et al., 2004; Warburton et al., 1997). This one-to-one correspondence with active, but not inactive, centromeres and the fact that it is a physical component of the chromosome both support the notion that CENP-A-containing centromeric chromatin, in turn, may specify the heritable epigenetic centromere.

Centromere inheritance after chromosome replication requires the replenishment of the epigenetic mark. This requires two critical components: (1) a physical mark at the centromere and (2) a *cis*-acting targeting element to guide newly made CENP-A to the centromere. CENP-A directs compaction and conformational rigidity to the subnucleosomal tetramer it makes with histone H4 (Black et al., 2004) relative to the corresponding tetramers of histones H3 and H4. This structural alteration would lie within the core of the nucleosome and may potentially differentiate centromeric chromatin from the rest of the chromosome. The region within the histone fold domain of CENP-A that may provide the basis for this physical centromere mark also serves as the *C*ENP-*A* *t*argeting *d*omain (or CATD). A subnucleosomal tetramer assembled by using H3^{CATD}, a chimeric histone H3 that contains the CATD (consisting of the loop 1 and α2 helix from CENP-A), and histone H4 adopts the more compact conformation of the (CENP-A/H4)$_2$ tetramer and is faithfully assembled into centromeric chromatin (Black et al., 2004).

We now use genetic replacement involving sequential and stable, transcription-mediated RNAi in human cells and plasmid shuffle in budding yeast to test the model of CENP-A and its CATD as the generators of conformationally distinct nucleosomes sufficient to maintain centromere assembly and replication.

RESULTS

H3^{CATD} Maintains Centromere Function upon CENP-A Depletion

To determine the abundance of CENP-A at the 1–10 megabase human centromeres (Willard and Waye, 1987), immunoblotting of extracts from randomly cycling HeLa cells was performed with known amounts of CENP-A as quantitation standards. This revealed that CENP-A is normally present at ~3 ng in 5 × 10^4 HeLa cells (Figure 1C), which equates to 2 × 10^6 copies per cell or 3 × 10^4 copies per centromere (taking into account a DNA content of ~50 chromosomes in these cells [Kops et al., 2004] with ~60% of cells in G1, ~20% in S phase, and ~20% in G2/M). Therefore, an average centromere contains at most 30,000 CENP-A molecules or 15,000 CENP-A-containing nucleosomes covering a total of 2.5 megabases of 171 bp α satellite repeats. To test if targeting histone H3 to centromeres could functionally replace the thousands of CENP-A molecules in these nucleosomes, stable cell lines were generated that accumulated centromere-bound yellow fluorescent protein (YFP)-tagged histone H3 substituted with the 22 amino acid changes in loop 1 and the α2 helix of CENP-A that form the CATD (Figures 1A and 1B). Two of the resultant YFP-H3^{CATD}-expressing lines were found to contain respective molar ratios to endogenous CENP-A of ~1.2 (Figure 1C, lane 1) and ~0.6 (Figure 1C, lane 2).

In the highest expressing line (with sufficient YFP-H3^{CATD} to replace the entire pool of endogenous CENP-A), stable transfection with a hygromycin-selectable transcription-mediated siRNA was then used to chronically lower CENP-A synthesis. Reduction of CENP-A eliminated colony outgrowth in almost all control, YFP-H3-expressing HeLa cells lacking the centromere-targeted H3^{CATD} rescue construct (Figure 1D). The few surviving individual colonies after CENP-A-directed RNAi in YFP-H3-expressing cells survived by escaping knockdown, with undiminished CENP-A levels (Figure S1 in the Supplemental Data available with this article online). However, two-thirds (64%) of YFP-H3^{CATD}-expressing cells retained colony-forming ability despite reduction in CENP-A levels. Individual colonies were recovered from a parallel set of plates and expanded to produce stable cell lines, and CENP-A level was determined. Sixteen of twenty-one colonies examined had CENP-A levels reduced by 3-fold (Figure 1E; data not shown) (with the remaining five escaping CENP-A reduction). YFP-H3^{CATD} is thus sufficient to

(F) YFP-H3^{CATD} performs an essential function when CENP-A levels are lowered. Parental cells expressing YFP-H3^{CATD} over the background of endogenous CENP-A form colonies in the absence or presence of YFP-directed RNAi. Cell lines with reduced levels of CENP-A are highly sensitive to subsequent reduction of YFP-H3^{CATD} levels.

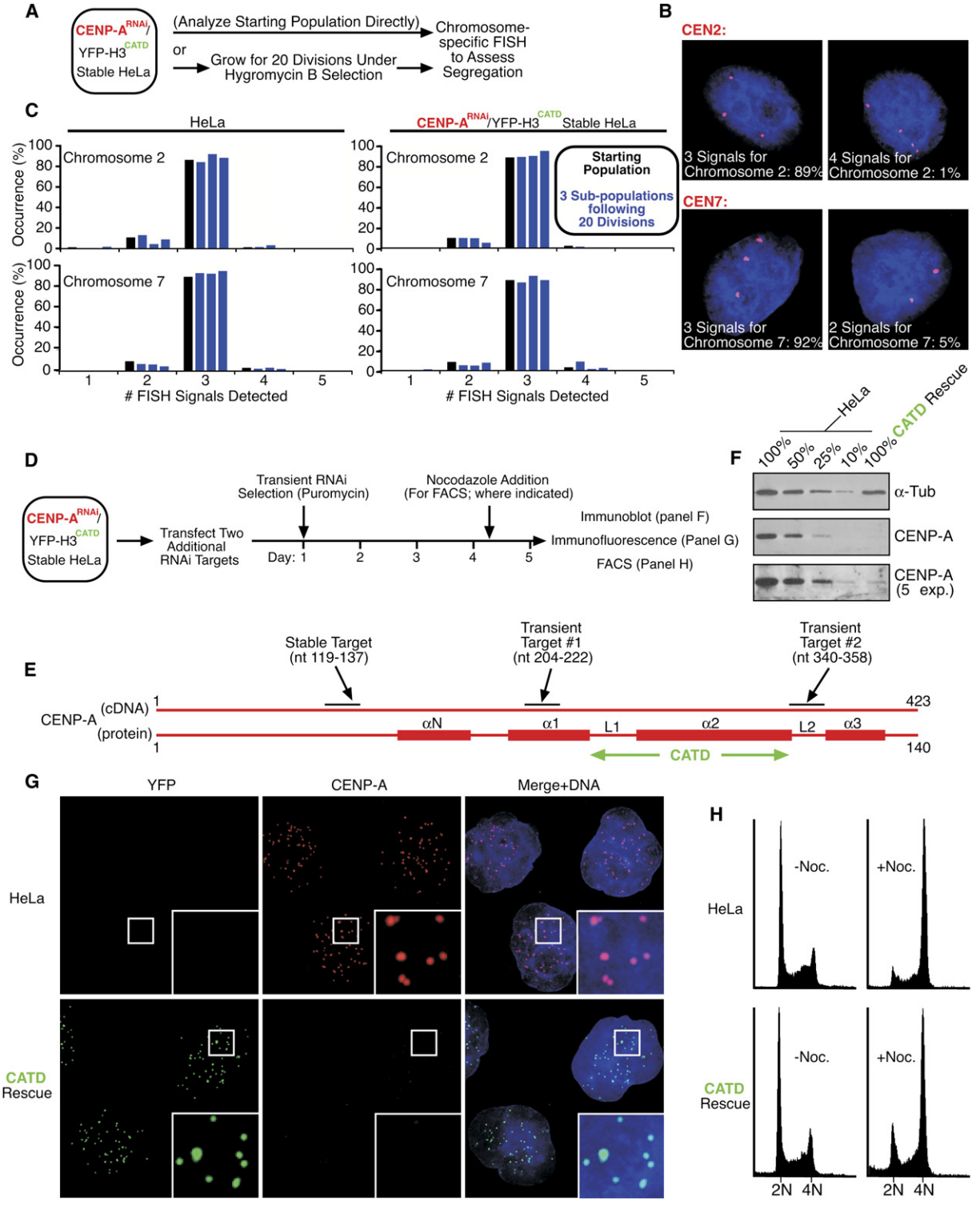

Figure 2. Functional Centromeres upon Depletion of CENP-A in YFP-H3^{CATD}-Expressing Cells

(A) Scheme for FISH experiment to address chromosome segregation fidelity. Cells stably expressing both YFP-H3^{CATD} and CENP-A-directed RNAi or parental HeLa cells were fixed and subjected to FISH for centromere regions of chromosomes 2 and 7 (CEN2 and CEN7, respectively) either directly or after allowing cells to propagate for 20 divisions.

(B) Representative images of CENP-A-^{RNAi}/YFP-H3^{CATD} cells hybridized with the indicated probe. The percentages of occurrence of centromere signals are from line #3 after 20 divisions.

increase cell viability after significant, long-term reduction of CENP-A.

H3CATD-Mediated Maintenance of Centromere Function Can Replace CENP-A

To determine if YFP-H3CATD in cells with reduced CENP-A was responsible for retention of viability, its level was reduced by stable, transcription-mediated siRNA targeted to sequences within the YFP moiety (Figure 1F). Although parental cell lines expressing YFP-H3CATD and normal levels of endogenous CENP-A produced a large number of colonies upon selection for the YFP-targeted RNAi plasmid, fewer than 1 in 100 cells with reduced CENP-A levels (from two independently isolated cell lines, Figure 1F and data not shown) retained the ability to grow sufficiently well to form colonies once YFP-H3CATD was reduced. Thus, H3CATD is sufficient to rescue an essential function of CENP-A at the centromere when CENP-A levels are reduced.

We tested whether YFP-H3CATD in these cells with reduced CENP-A could restore accurate chromosome segregation by measuring karyotypic stability through 20 cell generations (Figure 2A). Chromosome copy numbers for chromosomes 2 and 7 were monitored by fluorescence in situ hybridization (FISH). Both the YFP-H3CATD cells with chronic reduction of CENP-A as well as parental HeLa cells (which maintain three copies of each FISH signal in ~90% of the HeLa cell population) displayed similar distributions of chromosome numbers for both chromosomes 2 and 7 (Figures 2B and 2C). The distribution of copy numbers for each of these two chromosomes did not change significantly over the course of a 20 generation culture period in either the YFP-H3CATD cells with critically reduced CENP-A levels or in parental HeLa cells. Chromosome segregation fidelity in cells in which the essential CENP-A function is provided by YFP-H3CATD (Figure 1F) is thus maintained over long durations of mitotic growth (Figures 2A–2C).

To address whether H3CATD could functionally replace the entire pool of CENP-A in cell lines already stably depleted to ~30% of normal CENP-A protein levels (Figure 1E), the remaining pool of endogenous CENP-A was further reduced by an additional transfection and selection (with puromycin) for transcription-based siRNA against two additional sites within the CENP-A mRNA (Figures 2D and 2E). Within 5 days, this produced cells that were depleted by 90% of endogenous CENP-A (Figure 2F) and in which YFP-H3CATD remained properly targeted to centromeric foci (Figure 2G). Centromere function was apparently not compromised in these H3CATD-expressing cells depleted of most endogenous CENP-A, because under typical growth conditions they maintained a normal cell-cycle profile and centromere-dependent mitotic checkpoint signaling remained intact as judged by mitotic arrest after addition of a microtubule-assembly disruptor (Figure 2H).

Rescue of Mitotic Kinetochore Function by H3CATD

Kinetochore assembly was also assessed in more detail in CENP-A-depleted mitotic cells rescued by H3CATD. The inner kinetochore component CENP-C has been found in diverse eukaryotes to require CENP-A for its centromere association (Goshima et al., 2003; Heeger et al., 2005; Howman et al., 2000; Oegema et al., 2001; Regnier et al., 2005). In cells with H3CATD (which has no sequences similar to the CENP-A tail) replacing >90% of CENP-A, CENP-C assembly at kinetochores was undiminished (Figure 3B). The centromere staining of the alphoid DNA binding component CENP-B becomes less compact upon reduction of CENP-A by gene targeting in mouse embryos, consistent with a perturbation in centromeric chromatin structure (Howman et al., 2000). However, replacement of CENP-A with the chimeric H3CATD maintained underlying centromeric chromatin with undiminished CENP-B binding (Figure S2A). Aurora B, another inner centromere protein and a component of the survivin-containing passenger protein complex, has been proposed to be recruited to centromeres by CENP-A (Kunitoku et al., 2003; Liu et al., 2006). However, others have reported that recruitment of Aurora B occurs independently of CENP-A (Oegema et al., 2001; Regnier et al., 2005). In either case, it too bound to CENP-A-depleted, H3CATD-containing kinetochores as well as it did to normal kinetochores (Figure S2C). So too did outer kinetochore components, including CENP-E (Figure 3C) and the mitotic checkpoint component Mad2 (Figure S2B).

Functionality of CENP-A-depleted kinetochores rescued by H3CATD was directly examined by following mitotic progression in live cells in which chromosome movements could be followed after cotransfection of a plasmid expressing histone H2B-mRFP along with siRNA

(C) Chromosome counts for each probe in initial cultures (black) and in three independently cultured populations (blue) grown for 20 divisions from the initial culture. >300 cells were scored for each parental HeLa (left) and the CENP-ARNAi/YFP-H3CATD cells (right) for both chromosomes 2 (top) and 7 (bottom).
(D) Scheme for experiments to analyze mitotic behavior and kinetochore status of YFP-H3CATD-expressing cells upon CENP-A depletion.
(E) Targets for sequential knockdown approach to deplete CENP-A.
(F) Immunoblot to assess the level of CENP-A depletion. Cells were treated as outlined in (D) and loaded adjacent to a dilution series of parental HeLa cells (see indicated percentage of cells loaded in relation to the CATD rescue cells). Stable selection of the plasmid led to a pool of cells with detectable CENP-A (Figure S4A). This reemergence of CENP-A expression occurs either through inactivation of the RNAi itself, a diminution of RNAi expression, or another form of escape from expression of RNAi (note that a similar reemergence of YFP expression occurs in a parental cell line that does not rely upon YFP expression for viability [Figure S4B]).
(G) Immunofluorescence of CENP-A in CATD rescue cells (bottom row).
(H) FACS analysis shows that CATD rescue cells mount a mitotic checkpoint in response to the microtubule poison nocodazole (Noc.).

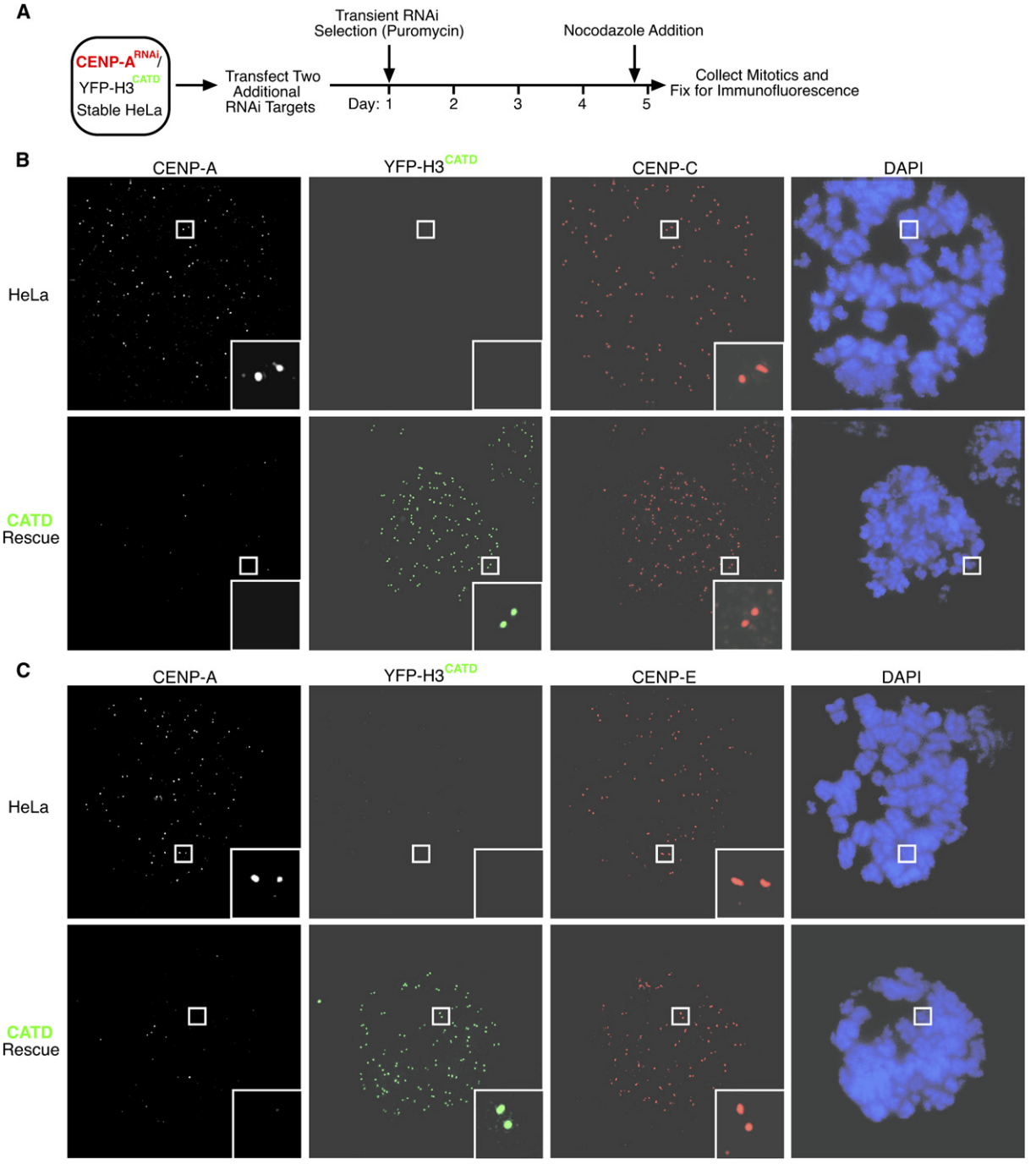

Figure 3. Intact Kinetochores in YFP-H3^{CATD}-Expressing Cells upon Depletion of CENP-A

(A) Scheme for analysis of mitotic kinetochores in CATD rescue cells.

(B and C) CENP-C ([B], red), an inner kinetochore component, and CENP-E ([C], red), an outer kinetochore component, are localized properly on mitotic kinetochores in CATD rescue cells.

plasmids to diminish CENP-A (Figure 4A). In control cells expressing YFP-H3, CENP-A levels were reduced to below detection limits at most mitotic kinetochores within 3 days (Figure 4B, second row from top). Partial depletion of CENP-A yielded severely lagging chromosomes in anaphase (Figure 4C, second row from top; Movie S2), indicative of a defect in kinetochore assembly and microtubule attachment. Using the sequential CENP-A knockdown approach in cells initially rescued by YFP-H3^{CATD}, CENP-A depletion did not disturb normal mitotic progression by

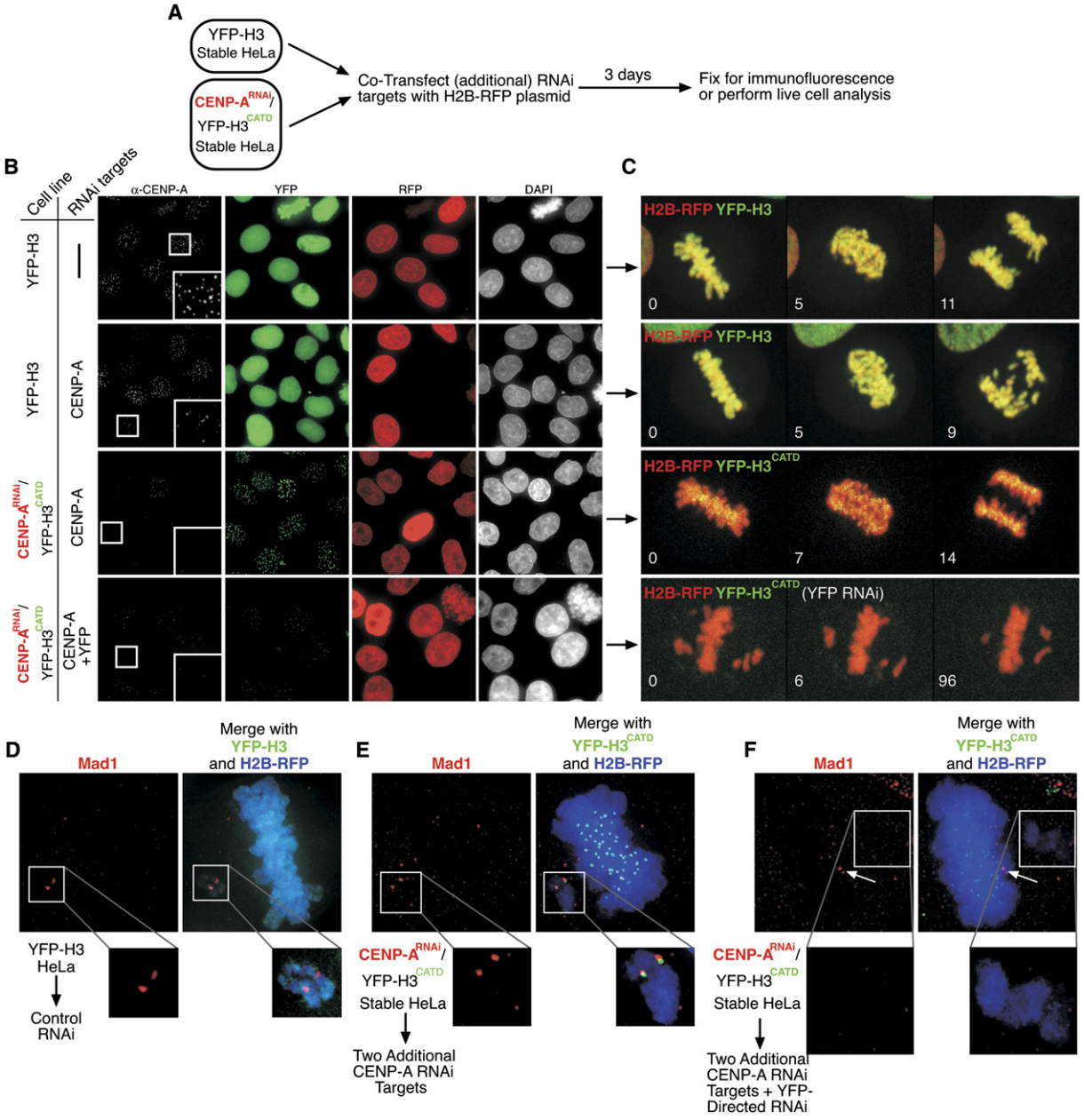

Figure 4. H3CATD-Mediated Rescue Is Essential for Proper Kinetochore Function during Mitosis

(A) Scheme for cotransfection approach to examine H3CATD-mediated rescue in living cells.

(B) Analysis of CENP-A knockdown by cotransfection of the indicated cocktails of RNAi plasmids and a cotransfection marker plasmid expressing RFP-tagged histone H2B. The sequential knockdown approach to depleting CENP-A leads to the most dramatic reduction in CENP-A levels (third row from top). In addition, both CENP-A and YFP-H3CATD are removed by using a cocktail that includes RNAi-expressing plasmids targeting both CENP-A and the YFP moiety of YFP-H3CATD (bottom row).

(C) Mitotic behavior was monitored by live cell microscopy in each of the conditions indicated in (B).

(D–F) To examine the spindle checkpoint under the various RNAi treatments, cells were treated as in (A) and processed for Mad1 immunolocalization. Both control YFP-H3 cells with a control RNAi vector (D) and YFP-H3CATD-expressing "CATD rescue" cells (E) have high levels of Mad1 on the kinetochores of unaligned chromosomes in late prometaphase. Cells simultaneously depleted of both CENP-A and H3CATD contain unaligned chromosomes that are defective in recruiting Mad1 (F). Partially functioning kinetochores that have congressed exhibit misattachment to the spindle, and these kinetochores recruit high levels of Mad1 (arrows).

any measure: chromosome motility during congression occurred with normal velocity (1.07 ± 0.53 μm/min versus 1.02 ± 0.39 μm/min in control cells), all chromosomes aligned prior to anaphase onset (Figure 4C, third row from top; Movies S3 and S4), and anaphase chromosome-to-pole movements were normal (0.77 ± 0.32 μm/min versus 0.84 ± 0.18 μm/min in control cells). Normal kinetochore function in CENP-A-depleted cells required the H3^{CATD}, because its removal by RNAi targeted to its YFP sequences (Figure 4B, bottom row) produced failure of congression with a subset of chromosomes misaligned for an extended, preanaphase period (Figure 4C, bottom row; >96 min; Movie S5). Although congression failure is the predominant phenotype upon codepletion of CENP-A and YFP-H3^{CATD}, we also observed lagging chromosomes upon attempting to separate chromosomes in anaphase (Figure S3 and Movie S6).

The extended mitotic delay seen upon simultaneous depletion of endogenous CENP-A and the rescuing H3^{CATD} was unexpected, as loss of CENP-A function at the level of an individual kinetochore was predicted to disrupt recruitment of components of the kinetochore-dependent mitotic checkpoint signaling formation that are required for generating the delay. A single unattached kinetochore in the parental CENP-A-containing cells is capable of producing a sufficient level of the checkpoint inhibitor to delay transition to anaphase (Bomont et al., 2005; Rieder et al., 1995). Checkpoint signaling at individual kinetochores is provided by recruitment of checkpoint components, including a complex containing Mad1 and Mad2, both of which are released from kinetochores as the checkpoint is silenced by spindle microtubule capture (Shah et al., 2004). As expected, in control cells, high levels of Mad1 were found on unattached kinetochores (Figure 4D) but were absent after alignment. Consistent with the observed mitotic arrest, CENP-A-depleted/H3^{CATD}-rescue cells recruited comparable levels of Mad1 (Figure 4E) to unattached kinetochores, whereas none was detectable on aligned, bioriented chromosomes.

Simultaneous depletion of CENP-A and the rescuing H3^{CATD} resulted in a subset of chromosomes that did not attach, all of which failed to recruit detectable Mad1 (Figure 4F), consistent with failure to assemble a kinetochore capable of either attaching to spindle microtubules or generating a mitotic checkpoint-mediated arrest. On the other hand, most chromosomes did congress (Figure 4F), indicating retention of at least partial function even after transient depletion of the majority of CENP-A and the rescuing H3^{CATD}. Despite alignment, some centromeres recruited levels of Mad1 comparable to those of unattached kinetochores in normal cells (Figure 4F, arrows). These Mad1-positive centromeres must, therefore, represent partially functional ones capable of attachment sufficient for initial congression and for arresting advance to anaphase by generation of mitotic checkpoint signaling, but for which attachment is unstable, thereby rerecruiting Mad1-dependent checkpoint signaling despite initial attachment.

Dissecting the CATD: Targeting Information in Loop 1 and α2 Helix of CENP-A

Loop 1 is critical for CENP-A targeting in both humans and flies because mutation in this region leads to mistargeting of CENP-A to chromosome arms (Black et al., 2004; Shelby et al., 1997; Vermaak et al., 2002). It is also a region of evolutionary hypervariability, insomuch as some related fruit fly species contain incompatible targeting residues within their respective loop 1 regions (Vermaak et al., 2002). Swapping loop 1 within the backbone of *D. bipectinata* CENP-A relative (called CID in fruit flies) with the corresponding loop 1 from *D. melanogaster* regenerates a CID molecule that is capable of targeting to *D. melanogaster* centromeres (Vermaak et al., 2002). Unlike the CATD (the combination of loop 1 and the adjacent α2 helix) that is able to convert histone H3 into a centromeric histone (Black et al., 2004), loop 1 alone is insufficient (Vermaak et al., 2002).

Deposition of histone H3.1 and H3.2 variants is coupled to replication, whereas the deposition of H3.3 is replication independent (Ahmad and Henikoff, 2002; Tagami et al., 2004; Worcel et al., 1978; Wu et al., 1982). The critical residues for the replication-dependent targeting of H3.1 and H3.2 correspond to S87, V89, and M90 within the α2 helix (Ahmad and Henikoff, 2002). The alteration of any of these residues allows for deposition of H3 outside of S phase, and in the case of the histone H3.3 variant that is deposited in a replication-independent manner (Ahmad and Henikoff, 2002; Tagami et al., 2004), all three of these residues are changed to A, I, and G, respectively (Figure 5A). Because these three residues are also each changed in CENP-A (Figure 5A), this suggests that the CATD may be comprised of two independent components: (1) targeting information within loop 1 and (2) residues within the α2 helix that direct the timing of CENP-A deposition, permitting replication-independent deposition of CENP-A, which is thought to occur during G2 (Shelby et al., 2000). To test this model, substitutions were made converting these sequences in CENP-A to either the replication-dependent H3.1 or H3.2 residues (Q_LL → S_VM) or the replication-independent H3.3 residues (Q_LL → A_IG). If the α2 helix is solely providing determinants permissive for deposition timing outside of S phase, CENP-A targeting should be maintained with alteration to the H3.3 residues but would mistarget with the H3.1/2 substitutions. In fact, both H3.1/2 and H3.3 substitutions resulted in the mistargeting of CENP-A (Figure 5B) or H3^{CATD} (Figure 5C) to chromosome arms.

An Analogous CATD in Budding Yeast CENP-A (Cse4p)

Our experiments in mammalian cells indicate that the information for both CENP-A localization and subsequent function (once assembled into centromeric chromatin) is provided by the CATD. Although CATD function is likely conserved in mammals (because the CENP-A-specific changes in its α2 helix that contact histone H4 are highly conserved), the generality of a CATD domain in supplying

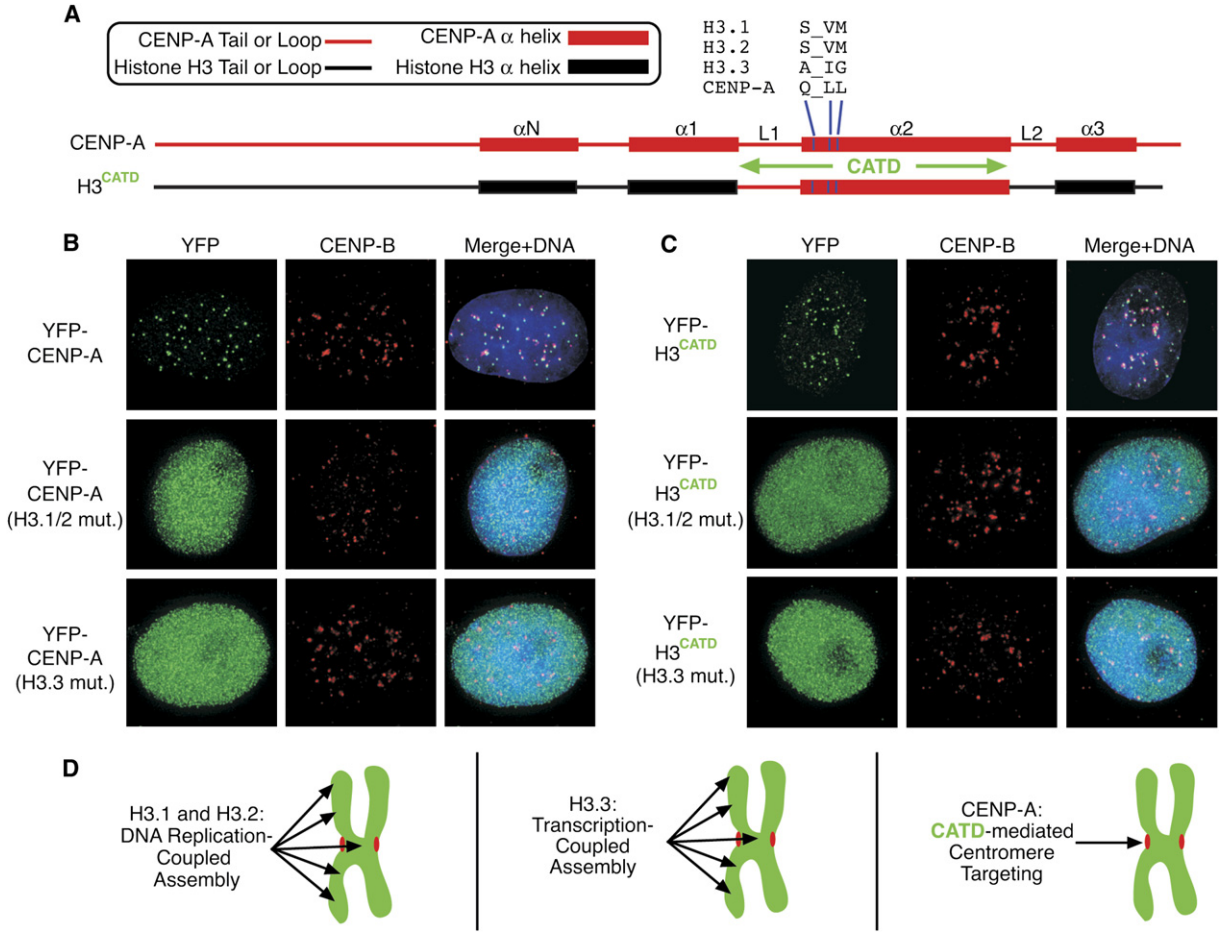

Figure 5. Replication Timing Determinants from H3.1/2 and H3.3 Are Each Incompatible with the Centromere Targeting of CENP-A

(A) Diagram of CENP-A and H3^{CATD}. The three blue bars represent the position of the residues that are critical for the replication-dependent assembly of H3.1 and H3.2 and the replication-independent assembly of H3.3 (Ahmad and Henikoff, 2002). The identities of these residues in each of the indicated H3 variants are listed above the diagram.

(B and C) CENP-A (B) and H3^{CATD} (C) are each mistargeted to noncentromeric chromatin upon substitution with either H3.1/2 or H3.3 residues at the positions highlighted in (A). Cells were fixed and processed for indirect immunofluorescence 2 days after transfection with plasmids expressing the indicated YFP-tagged proteins.

(D) Three distinct routes to chromatin assembly. See text for details.

the essential centromere function(s) of CENP-A was tested in budding yeast. In contrast to the megabase centromeres of mammals, the centromere of budding yeast contains only one or a few specialized nucleosomes containing the essential CENP-A ortholog Cse4p (Smith, 2002; Stoler et al., 1995), although this view is challenged by a recent report of a region of 20–40 kb surrounding the centromere with partial coverage by Cse4p-containing nucleosomes (Riedel et al., 2006). Cse4p differs from histone H3 within the CATD region by a similar number of amino acid insertions and substitutions as CENP-A does in mammals (18 out of 43 residues in Cse4p compared to 22 out of 42 residues in CENP-A), but most of the changes are themselves not conserved.

We tested if in the complete absence of Cse4p the corresponding region of Cse4p forms a functional CATD in this strikingly small centromere. The endogenous *CSE4* locus was deleted, and centromere function was supported by an ectopic copy of *CSE4* residing on a *URA3*-encoding plasmid. These cells were transformed with a second plasmid carrying various potential rescue constructs (Figure 6A) expressed under the control of a *GAL1* promoter. Because loss of the Cse4p encoding plasmid can be counterselected by using 5-fluoroorotic acid (5FOA), such plasmid shuffling was used to test for the ability to grow in the absence of *CSE4*. As suggested by previous mutagenesis studies (Keith et al., 1999), a successful H3/Cse4p chimeric protein required specific N-terminal and C-terminal features from Cse4p for centromere function (Figure 6A). The N terminus of Cse4p is substantially larger than that of CENP-A (129 versus 40 amino acids). Although its structure is unknown, it contains a 33

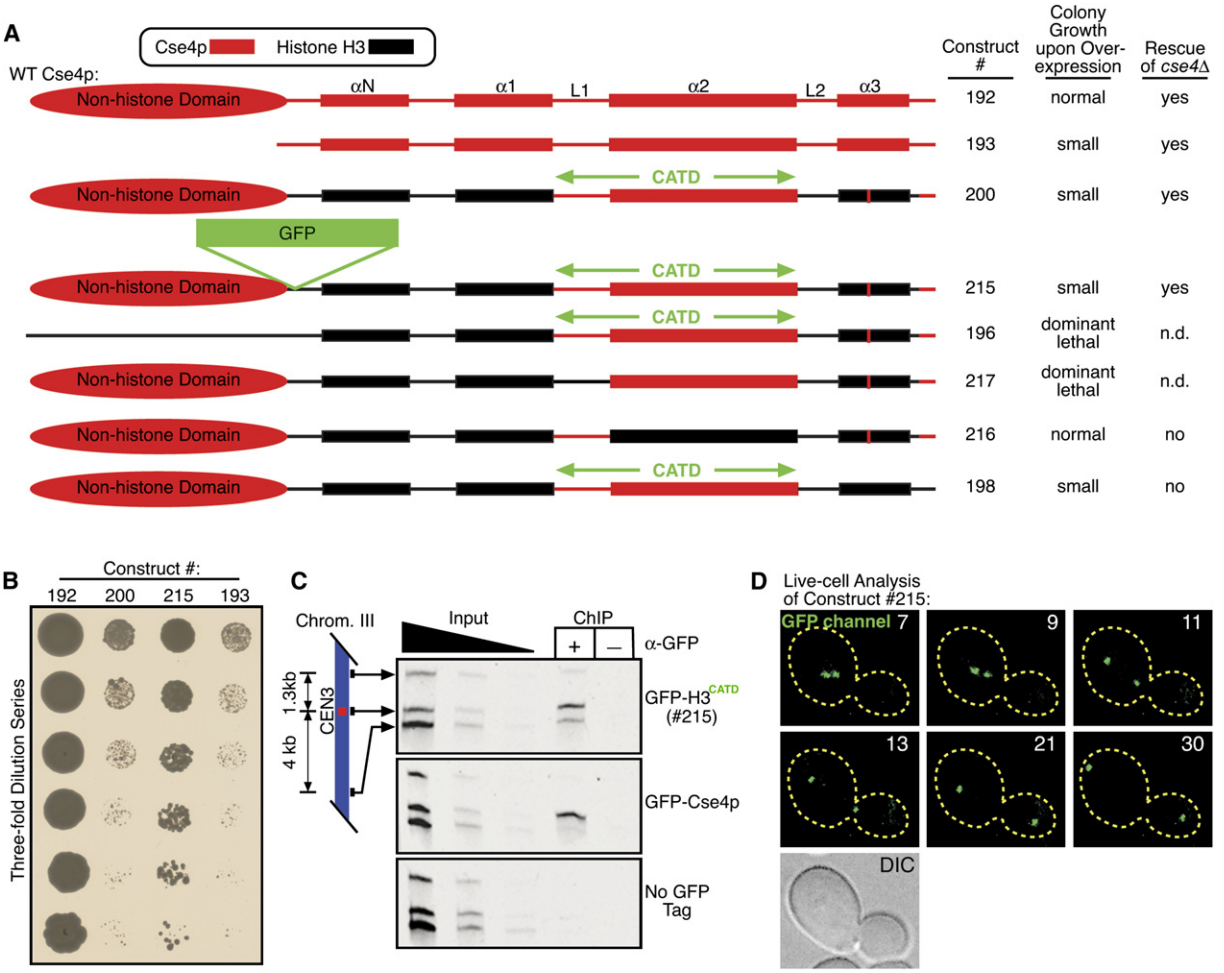

Figure 6. CATD Function in Budding Yeast

(A) Diagrams and behavior of potential *CSE4* rescue constructs for galactose-induced expression. See Figure S5 for immunoblotting.

(B) Rescue of *cse4Δ* by either full-length Cse4p (#192), the histone fold domain of Cse4p alone (#193), or by CATD-containing rescue constructs (#200 is untagged and #215 contains a GFP tag). A dilution series is shown for each strain.

(C) GFP-H3^{CATD} (#215) is enriched at the centromere by ChIP. GFP-Cse4p (middle) is included as a control.

(D) Mitotic behavior of the CATD-containing rescue construct in live cells. The construct localizes to centromeric clusters that are segregated to both mother and daughter cells in mitosis.

amino acid domain that is not conserved, termed END, which has been proposed to be an interaction interface with components of the budding yeast kinetochore (Chen et al., 2000). The extreme C-terminal residues of Cse4p are also not conserved but are positioned at the contact site with its partner Cse4p molecule in a putative homotypic centromeric nucleosome at the budding yeast centromere.

To identify the minimal yeast CATD sequence, a series of six hybrid genes encoding histone H3 substituted with portions of *CSE4* was constructed (Figure 6A). As is also the case in humans (Black et al., 2004; Shelby et al., 1997), a minimal CATD was identified to consist of both the loop 1 and α2 helix. Both were necessary for centromere function in yeast, with constructs lacking either region of Cse4p (#217 and 216, Figure 6A) unable to replace *CSE4* function. Yeast containing this H3^{CATD}, either alone (strain #200) or with GFP inserted between the histone fold domain (strain #215) and the N-terminal nonhistone domain, restored viability to *cse4Δ* cells (Figure 6B). Chromatin immunoprecipitation (ChIP) of GFP-H3^{CATD} verified its specific localization at the centromere (using antibodies to GFP and primers for CEN3; Figure 6C), just as is seen for Cse4p (Figure 6C) (as previously reported; [Meluh et al., 1998]). Live cell imaging of yeast supported only by H3^{CATD} revealed continued clustering of discrete centromeric foci whose behavior throughout mitosis mirrored that of strains with authentic Cse4p (Figure 6D and Movie S7).

DISCUSSION

Our findings with human cells and budding yeast demonstrate that the function of the CATD is conserved from fungi to mammals and support the notion that it acts from within the octameric core of the centromeric nucleosome to specify the location for kinetochore assembly. The replacement of CENP-A with a histone H3 chimera containing the 22 amino acid substitutions that generate the CATD demonstrates that the major, possibly sole, function of the specialized centromeric nucleosome is to generate a unique chromatin environment. The CATD targets newly made CENP-A (or H3^{CATD}) to the centromere, possibly altering the structure of the nucleosomes into which it assembles. As opposed to histone tails that are used to modulate histone function in diverse chromatin-mediated processes, the CATD affects CENP-A function from within the histone fold that is predicted to be buried within the nucleosome core (Black et al., 2004). In our replacement in human cells, H3^{CATD} retains the amino-terminal tail from canonical H3 but still yields proper targeting of CENP-C to centromeres in the absence of the CENP-A amino-terminal tail (Figure 3B). With inner centromere components (such as Aurora B) and inner kinetochore components (such as CENP-B and CENP-C) still targeted, the H3^{CATD} replacement centromeres form a functional kinetochore with the outermost class of proteins involved in mediating and sensing microtubule attachment (represented in our experiments by CENP-E [Figure 3C], Mad1 [Figure 4F], and Mad2 [Figure S2B]) recruited at normal levels.

Deposition Pathway for CENP-A Is Distinct from H3.1/2 and H3.3

A consequence of the location of the CATD, which overlaps with the position of the residues (Ahmad and Henikoff, 2002) that direct the DNA replication-dependent loading of H3.1 by the CAF-1 complex (Smith and Stillman, 1989; Tagami et al., 2004), is that it allows CENP-A to be loaded outside of S phase. The H3.3-specific amino acid substitutions dictate its own replication-independent recognition by the HIRA complex and subsequent loading onto chromosomes (Ahmad and Henikoff, 2002; Tagami et al., 2004), and this loading has been proposed to be linked to transcription (Chow et al., 2005; Mito et al., 2005; Schwartz and Ahmad, 2005; Wirbelauer et al., 2005). Along with our analysis of the corresponding position of the H3 deposition determinants within the CATD of CENP-A, these earlier efforts support the notion that the depositions of H3.1/2 and H3.3 are not targeting events per se, but rather nontargeted events that are coupled to DNA metabolism (replication and transcription, respectively; Figure 5D). CENP-A deposition, however, operates independent of DNA sequence but must be a directed targeting. This is mediated by the CATD, which produces conformationally more rigid subnucleosomal tetramers of CENP-A and histone H4 (Black et al., 2004).

Specialized Nucleosomes as the Basis for Kinetochore Forming Centromeric Chromatin

Taking into account both the conformational rigidity conferred to the subnucleosomal tetramers by the CATD and the current functional data, we propose that a conformational difference conferred by the CATD serves as the initial determinant for chromatin loading (possibly involving an as yet unidentified chromatin loader) or stabilization after loading and as a final mark of specialized chromatin. The latter role in marking the chromatin would provide the physical basis for how centromeres are epigenetically specified. Determining the conformational flexibility or rigidity of these nucleosomes will be the critical test of this model. If CENP-A does indeed generate structurally divergent nucleosomes, once assembled, this unusual chromatin domain first recruits essential, constitutive centromere components, including the CENP-A nucleosome-associated complex (CENP-A^{NAC}) (Foltz et al., 2006) (comprised of six components, including CENP-C, CENP-H, CENP-M, CENP-N, CENP-T, and CENP-U[50]), CENP-I, and other proteins that form the inner kinetochore and in turn are thought to recruit outer kinetochore components that arrive at the centromere during prophase and prometaphase (Figure 7A).

A functional mammalian kinetochore likely requires the establishment of a localized array of CENP-A-containing nucleosomes because transiently forcing CENP-A to intersperse randomly into chromosome arms by transient overexpression did not produce spontaneous kinetochore formation at noncentromeric loci (Van Hooser et al., 2001). This view should be tempered by the report (in *D. melanogaster*) that expression of CID to 70-fold over its typical level (i.e., near the level of histone H3) yielded replacement of H3-containing nucleosomes in euchromatic regions, and this was coincident with occasional recruitment of one or more kinetochore components (Heun et al., 2006). What our evidence adds to this is that full centromere function is dependent upon the chromatin structure alteration that is mediated by the CATD. The structured core of histones is in contrast to their unstructured "tails" that protrude from the nucleosomal core. Although an auxiliary role of the CENP-A tail or CENP-A-specific tail modifications in HeLa cells cannot be eliminated, our finding that H3^{CATD} replacement is essential when CENP-A is substantially reduced indicates that if the structurally distinct core of CENP-A is embedded in centromeric nucleosomes then either tail will suffice. Furthermore, the essential role of the CATD in CENP-A function in the context of the array these nucleosomes formed at the centromere supports the hypothesis that the higher-order chromatin structure at the base of the kinetochore has its foundation in individual CENP-A-containing nucleosomes.

Higher-Order Chromatin Structure at the Inner Kinetochore

Although the higher-order organization of centromeric chromatin is thought to contain an array of CENP-A-containing nucleosomes that are not contiguous on physically

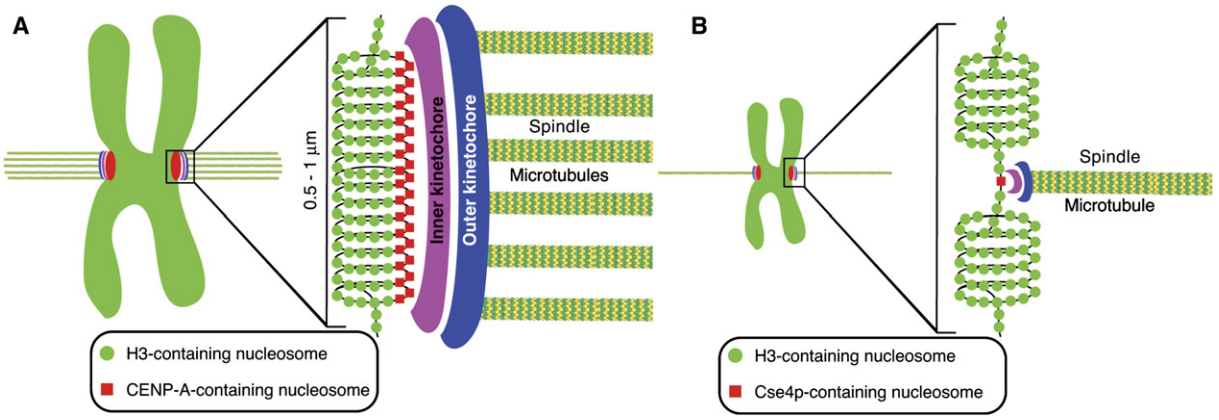

Figure 7. Centromeric Chromatin from Mammals to Budding Yeast
Diagrams for the organization and mitotic kinetochore function of structurally distinct nucleosomes containing CENP-A found exclusively at active mammalian (A) and budding yeast (B) centromeres. See text for details.

stretched chromatin fibers but are brought together in three-dimensional space (Blower et al., 2002; Zinkowski et al., 1991), the basis for this higher-order organization is unknown. During interphase, human centromeres exist as discrete subnuclear foci and remain associated after duplication in S phase. In prophase, as the chromatin condenses, CENP-A-containing chromatin is positioned at the exterior face of the chromosome in order to be in proper position to build a kinetochore that can attach to the bipolar spindle (Figure 7A). The kinetochore-forming CENP-A chromatin exists as a disk shape of ~0.5–1 μm in diameter that is thought to exclude H3-containing nucleosomes (Blower et al., 2002; Rieder, 1982). Our finding that there are sufficient protein levels to generate ~15,000 copies of the CENP-A-containing nucleosome at an average centromere leads to a model where this chromatin structure would contain one to two layers of CENP-A nucleosomes (Figure 7A). This higher-order chromatin structure at the mega multisubunit mammalian centromere is in contrasting size to the tiny centromeres of budding yeast, but each contains the rigid, centromere-specific nucleosome at the foundation of the kinetochore (Figure 7B).

All of this leads to a model for CATD-mediated targeting of newly made CENP-A that involves a self-directing process wherein the structurally distinct prenucleosomal complex of CENP-A/histone H4 tracks to existing CENP-A-templated chromatin and is assembled at immediately adjacent sites. Because the H3^{CATD} chimeric histone is sufficient to rescue CENP-A depletion in creating the underlying chromatin required for a functional inner kinetochore, this supports the view that the higher-order, three-dimensional organization of kinetochore-forming centromeric chromatin is also driven by self-directed interactions between uniquely structured nucleosomes. This would provide an explanation for neocentromere formation, with the earliest events involving the misincorporation of CENP-A at noncentromeric regions. After prolonged overexpression of CENP-A (colorectal cancer examples; [Tomonaga et al., 2003]) or under high selective pressure (neocentromere formation on marker chromosomes; [Depinet et al., 1997; du Sart et al., 1997; Warburton et al., 1997]), the self-association between adjacent nucleosomes creates a chromatin environment that is conducive to expanding and propagating the region. Thus, a new centromere is formed and, in the case of a heritable neocentromere, is epigenetically maintained. This model places the centromere-specific nucleosome as the fundamental chromatin unit driving centromere inheritance and establishing the site for kinetochore assembly.

EXPERIMENTAL PROCEDURES

Plasmid-Based RNAi

RNAi experiments were performed in HeLa cells or their derivatives stably expressing the indicated YFP fusion proteins. RNAi target sequences were expressed from transfected, selectable plasmids. Details regarding the generation of the cell lines, RNAi target sequences, viability assays, and analysis by immunoblot, immunofluorescence, FACS, and FISH can be found in the Supplemental Data.

CSE4 Gene Replacement

Plasmid shuffling was used to replace CSE4 with the indicated inducible constructs, and growth was assessed by using 5FOA-mediated counter-selection. Details regarding strains, constructs, the plasmid shuffle scheme, growth tests, and ChIP analysis can be found in the Supplemental Data.

Live Cell Analysis

Both mammalian cells and yeast cells were analyzed in mitosis by using a spinning disk confocal microscope. Images were acquired in the GFP, YFP, and/or RFP channels, where indicated, as well as by differential interference contrast. Details regarding growth conditions, microscopy, and image capture can be found in the Supplemental Data.

Supplemental Data

Supplemental Data include Supplemental Experimental Procedures, Supplemental References, five figures, and seven movies and can be found with this article online at http://www.molecule.org/cgi/content/full/25/2/309/DC1/.

ACKNOWLEDGMENTS

We thank G. Kops (UCSD) and I. Cheeseman (UCSD) for helpful discussions, R. Tsien (UCSD), K. Yoda (Nagoya), B. Earnshaw (Edinburgh), K. Sullivan (Scripps), B. Weaver (UCSD), R. Kolodner (UCSD), K. Monier (Lyon), and A. De Antoni and A. Musacchio (Milan) for generously providing reagents, and D. Young (UCSD Flow Cytometry) for sorting cells. Some images were acquired at the UCSD Neuroscience Microscope Shared Facility (Supported by National Institute of Neurological Disorders and Stroke). This work was supported by grants from the National Institutes of Health to D.W.C. B.E.B. was supported by a postdoctoral fellowship from the American Cancer Society and a Career Award in the Biomedical Sciences from the Burroughs Wellcome Fund, and L.E.T.J. was supported by a postdoctoral fellowship from Philip Morris USA Inc. Salary support for D.W.C. and A.B.D. is provided by the Ludwig Institute for Cancer Research.

Received: March 9, 2006
Revised: June 13, 2006
Accepted: December 20, 2006
Published: January 25, 2007

REFERENCES

Ahmad, K., and Henikoff, S. (2002). The histone variant H3.3 marks active chromatin by replication-independent nucleosome assembly. Mol. Cell *9*, 1191–1200.

Amor, D.J., Bentley, K., Ryan, J., Perry, J., Wong, L., Slater, H., and Choo, K.H. (2004). Human centromere repositioning "in progress". Proc. Natl. Acad. Sci. USA *101*, 6542–6547.

Black, B.E., Foltz, D.R., Chakravarthy, S., Luger, K., Woods, V.L., and Cleveland, D.W. (2004). Structural determinants for generating centromeric chromatin. Nature *430*, 578–582.

Blower, M.D., Sullivan, B.A., and Karpen, G.H. (2002). Conserved organization of centromeric chromatin in flies and humans. Dev. Cell *2*, 319–330.

Bomont, P., Maddox, P., Shah, J.V., Desai, A.B., and Cleveland, D.W. (2005). Unstable microtubule capture at kinetochores depleted of the centromere-associated protein CENP-F. EMBO J. *24*, 3927–3939.

Chen, Y., Baker, R.E., Keith, K.C., Harris, K., Stoler, S., and Fitzgerald-Hayes, M. (2000). The N terminus of the centromere H3-like protein Cse4p performs an essential function distinct from that of the histone fold domain. Mol. Cell. Biol. *20*, 7037–7048.

Chow, C.M., Georgiou, A., Szutorisz, H., Maia e Silva, A., Pombo, A., Barahona, I., Dargelos, E., Canzonetta, C., and Dillon, N. (2005). Variant histone H3.3 marks promoters of transcriptionally active genes during mammalian cell division. EMBO Rep. *6*, 354–360.

Cleveland, D.W., Mao, Y., and Sullivan, K.F. (2003). Centromeres and kinetochores: from epigenetics to mitotic checkpoint signaling. Cell *112*, 407–421.

Depinet, T.W., Zackowski, J.L., Earnshaw, W.C., Kaffe, S., Sekhon, G.S., Stallard, R., Sullivan, B.A., Vance, G.H., Van Dyke, D.L., Willard, H.F., et al. (1997). Characterization of neo-centromeres in marker chromosomes lacking detectable alpha-satellite DNA. Hum. Mol. Genet. *6*, 1195–1204.

du Sart, D., Cancilla, M.R., Earle, E., Mao, J.I., Saffery, R., Tainton, K.M., Kalitsis, P., Martyn, J., Barry, A.E., and Choo, K.H. (1997). A functional neo-centromere formed through activation of a latent human centromere and consisting of non-alpha-satellite DNA. Nat. Genet. *16*, 144–153.

Earnshaw, W.C., and Migeon, B.R. (1985). Three related centromere proteins are absent from the inactive centromere of a stable isodicentric chromosome. Chromosoma *92*, 290–296.

Earnshaw, W.C., and Rothfield, N. (1985). Identification of a family of human centromere proteins using autoimmune sera from patients with scleroderma. Chromosoma *91*, 313–321.

Foltz, D.R., Jansen, L.E.T., Black, B.E., Bailey, A.O., Yates, J.R., 3rd, and Cleveland, D.W. (2006). The human CENP-A centromeric nucleosome-associated complex. Nat. Cell Biol. *8*, 458–469.

Goshima, G., Kiyomitsu, T., Yoda, K., and Yanagida, M. (2003). Human centromere chromatin protein hMis12, essential for equal segregation, is independent of CENP-A loading pathway. J. Cell Biol. *160*, 25–39.

Heeger, S., Leismann, O., Schittenhelm, R., Schraidt, O., Heidmann, S., and Lehner, C.F. (2005). Genetic interactions of separase regulatory subunits reveal the diverged Drosophila Cenp-C homolog. Genes Dev. *19*, 2041–2053.

Heun, P., Erhardt, S., Blower, M.D., Weiss, S., Skora, A.D., and Karpen, G.H. (2006). Mislocalization of the Drosophila centromere-specific histone CID promotes formation of functional ectopic kinetochores. Dev. Cell *10*, 303–315.

Howman, E.V., Fowler, K.J., Newson, A.J., Redward, S., MacDonald, A.C., Kalitsis, P., and Choo, K.H. (2000). Early disruption of centromeric chromatin organization in centromere protein A (Cenpa) null mice. Proc. Natl. Acad. Sci. USA *97*, 1148–1153.

Keith, K.C., Baker, R.E., Chen, Y., Harris, K., Stoler, S., and Fitzgerald-Hayes, M. (1999). Analysis of primary structural determinants that distinguish the centromere-specific function of histone variant Cse4p from histone H3. Mol. Cell. Biol. *19*, 6130–6139.

Kops, G.J., Foltz, D.R., and Cleveland, D.W. (2004). Lethality to human cancer cells through massive chromosome loss by inhibition of the mitotic checkpoint. Proc. Natl. Acad. Sci. USA *101*, 8699–8704.

Kunitoku, N., Sasayama, T., Marumoto, T., Zhang, D., Honda, S., Kobayashi, O., Hatakeyama, K., Ushio, Y., Saya, H., and Hirota, T. (2003). CENP-A phosphorylation by Aurora-A in prophase is required for enrichment of Aurora-B at inner centromeres and for kinetochore function. Dev. Cell *5*, 853–864.

Liu, S.T., Rattner, J.B., Jablonski, S.A., and Yen, T.J. (2006). Mapping the assembly pathways that specify formation of the trilaminar kinetochore plates in human cells. J. Cell Biol. *175*, 41–53.

Manuelidis, L., and Wu, J.C. (1978). Homology between human and simian repeated DNA. Nature *276*, 92–94.

Masumoto, H., Masukata, H., Muro, Y., Nozaki, N., and Okazaki, T. (1989). A human centromere antigen (CENP-B) interacts with a short specific sequence in alphoid DNA, a human centromeric satellite. J. Cell Biol. *109*, 1963–1973.

Meluh, P.B., Yang, P., Glowczewski, L., Koshland, D., and Smith, M.M. (1998). Cse4p is a component of the core centromere of Saccharomyces cerevisiae. Cell *94*, 607–613.

Mito, Y., Henikoff, J.G., and Henikoff, S. (2005). Genome-scale profiling of histone H3.3 replacement patterns. Nat. Genet. *37*, 1090–1097.

Murnane, J.P., and Sabatier, L. (2004). Chromosome rearrangements resulting from telomere dysfunction and their role in cancer. Bioessays *26*, 1164–1174.

Nasmyth, K. (2005). How do so few control so many? Cell *120*, 739–746.

Oegema, K., Desai, A., Rybina, S., Kirkham, M., and Hyman, A.A. (2001). Functional analysis of kinetochore assembly in Caenorhabditis elegans. J. Cell Biol. *153*, 1209–1226.

Ohzeki, J., Nakano, M., Okada, T., and Masumoto, H. (2002). CENP-B box is required for de novo centromere chromatin assembly on human alphoid DNA. J. Cell Biol. *159*, 765–775.

Palmer, D.K., and Margolis, R.L. (1985). Kinetochore components recognized by human autoantibodies are present on mononucleosomes. Mol. Cell. Biol. *5*, 173–186.

Regnier, V., Vagnarelli, P., Fukagawa, T., Zerjal, T., Burns, E., Trouche, D., Earnshaw, W., and Brown, W. (2005). CENP-A is required for

accurate chromosome segregation and sustained kinetochore association of BubR1. Mol. Cell. Biol. *25*, 3967–3981.

Riedel, C.G., Katis, V.L., Katou, Y., Mori, S., Itoh, T., Helmhart, W., Galova, M., Petronczki, M., Gregan, J., Cetin, B., et al. (2006). Protein phosphatase 2A protects centromeric sister chromatid cohesion during meiosis I. Nature *441*, 53–61.

Rieder, C.L. (1982). The formation, structure, and composition of the mammalian kinetochore and kinetochore fiber. Int. Rev. Cytol. *79*, 1–58.

Rieder, C.L., Cole, R.W., Khodjakov, A., and Sluder, G. (1995). The checkpoint delaying anaphase in response to chromosome monoorientation is mediated by an inhibitory signal produced by unattached kinetochores. J. Cell Biol. *130*, 941–948.

Schwartz, B.E., and Ahmad, K. (2005). Transcriptional activation triggers deposition and removal of the histone variant H3.3. Genes Dev. *19*, 804–814.

Shah, J.V., Botvinick, E., Bonday, Z., Furnari, F., Berns, M., and Cleveland, D.W. (2004). Dynamics of centromere and kinetochore proteins; implications for checkpoint signaling and silencing. Curr. Biol. *14*, 942–952.

Shelby, R.D., Vafa, O., and Sullivan, K.F. (1997). Assembly of CENP-A into centromeric chromatin requires a cooperative array of nucleosomal DNA contact sites. J. Cell Biol. *136*, 501–513.

Shelby, R.D., Monier, K., and Sullivan, K.F. (2000). Chromatin assembly at kinetochores is uncoupled from DNA replication. J. Cell Biol. *151*, 1113–1118.

Smith, M.M. (2002). Centromeres and variant histones: what, where, when and why? Curr. Opin. Cell Biol. *14*, 279–285.

Smith, S., and Stillman, B. (1989). Purification and characterization of CAF-I, a human cell factor required for chromatin assembly during DNA replication in vitro. Cell *58*, 15–25.

Stoler, S., Keith, K.C., Curnick, K.E., and Fitzgerald-Hayes, M. (1995). A mutation in CSE4, an essential gene encoding a novel chromatin-associated protein in yeast, causes chromosome nondisjunction and cell cycle arrest at mitosis. Genes Dev. *9*, 573–586.

Sullivan, B.A., Blower, M.D., and Karpen, G.H. (2001). Determining centromere identity: cyclical stories and forking paths. Nat. Rev. Genet. *2*, 584–596.

Sullivan, K.F. (2001). A solid foundation: functional specialization of centromeric chromatin. Curr. Opin. Genet. Dev. *11*, 182–188.

Sullivan, K.F., Hechenberger, M., and Masri, K. (1994). Human CENP-A contains a histone H3 related histone fold domain that is required for targeting to the centromere. J. Cell Biol. *127*, 581–592.

Tagami, H., Ray-Gallet, D., Almouzni, G., and Nakatani, Y. (2004). Histone H3.1 and H3.3 complexes mediate nucleosome assembly pathways dependent or independent of DNA synthesis. Cell *116*, 51–61.

Tomonaga, T., Matsushita, K., Yamaguchi, S., Oohashi, T., Shimada, H., Ochiai, T., Yoda, K., and Nomura, F. (2003). Overexpression and mistargeting of centromere protein-A in human primary colorectal cancer. Cancer Res. *63*, 3511–3516.

Van Hooser, A.A., Ouspenski, I.I., Gregson, H.C., Starr, D.A., Yen, T.J., Goldberg, M.L., Yokomori, K., Earnshaw, W.C., Sullivan, K.F., and Brinkley, B.R. (2001). Specification of kinetochore-forming chromatin by the histone H3 variant CENP-A. J. Cell Sci. *114*, 3529–3542.

Ventura, M., Weigl, S., Carbone, L., Cardone, M.F., Misceo, D., Teti, M., D'Addabbo, P., Wandall, A., Bjorck, E., de Jong, P.J., et al. (2004). Recurrent sites for new centromere seeding. Genome Res. *14*, 1696–1703.

Vermaak, D., Hayden, H.S., and Henikoff, S. (2002). Centromere targeting element within the histone fold domain of Cid. Mol. Cell. Biol. *22*, 7553–7561.

Warburton, P.E., Cooke, C.A., Bourassa, S., Vafa, O., Sullivan, B.A., Stetten, G., Gimelli, G., Warburton, D., Tyler-Smith, C., Sullivan, K.F., et al. (1997). Immunolocalization of CENP-A suggests a distinct nucleosome structure at the inner kinetochore plate of active centromeres. Curr. Biol. *7*, 901–904.

Willard, H.F. (1985). Chromosome-specific organization of human alpha satellite DNA. Am. J. Hum. Genet. *37*, 524–532.

Willard, H.F., and Waye, J.S. (1987). Hierarchical order in chromosome-specific human alpha satellite DNA. Trends Genet. *3*, 192–198.

Wirbelauer, C., Bell, O., and Schubeler, D. (2005). Variant histone H3.3 is deposited at sites of nucleosomal displacement throughout transcribed genes while active histone modifications show a promoter-proximal bias. Genes Dev. *19*, 1761–1766.

Worcel, A., Han, S., and Wong, M.L. (1978). Assembly of newly replicated chromatin. Cell *15*, 969–977.

Wu, R.S., Tsai, S., and Bonner, W.M. (1982). Patterns of histone variant synthesis can distinguish G0 from G1 cells. Cell *31*, 367–374.

Zinkowski, R.P., Meyne, J., and Brinkley, B.R. (1991). The centromere-kinetochore complex: a repeat subunit model. J. Cell Biol. *113*, 1091–1110.

Molecular Cell, Volume *25*

Supplemental Data

Centromere Identity Maintained by Nucleosomes Assembled with Histone H3 Containing the CENP-A Targeting Domain

Ben E. Black, Lars E.T. Jansen, Paul S. Maddox, Daniel R. Foltz, Arshad B. Desai, Jagesh V. Shah, and Don W. Cleveland

Supplemental Experimental Procedures

Cell lines

HeLa cells and their derivatives were cultured in DMEM supplemented with 10% fetal bovine serum (FBS) or newborn calf serum. HeLa monoclonal cell lines expressing either YFP-H3 or YFP-H3^{CATD} were generated by stable integration via Moloney murine leukemia retroviral delivery. The YFP-H3 and YFP-H3^{CATD} constructs (Black et al., 2004) were each sub-cloned into the retroviral plasmid, pBABE-BLAST (Shah et al., 2004), and these were subsequently co-transfected using Fugene 6 (Roche, Indianapolis, IN) with the VSV-G pseudotyping plasmid into 293-GP cells (which express the retroviral *gag* and *pol* genes) to generate amphotropic retrovirus (Morgenstern and Land, 1990). Virus-containing supernatant was harvested two days following transfection, passed through a 0.45 μm filter, mixed with hexadimethrine bromide (Polybrene; 8 μg/ml), and then incubated with HeLa cells overnight. Blasticidin S (Calbiochem, San Diego, CA; 2.5 μg/ml) selection was introduced two days following infection and continued for two weeks. Cells stably expressing the YFP-fusion proteins were isolated and individually sorted into separate wells of a 96-well plate by flow cytometry (FACSVantage, BD Biosciences, San Jose, CA) or by plating at a limiting dilution (one cell per three wells). The resulting monoclonal lines were expanded and examined by

fluorescence microscopy to identify lines expressing the YFP-fusion protein. All YFP-fusion protein-expressing HeLa lines were maintained in blasticidin S (1 μg/ml).

Plasmid-based RNAi

All of the RNAi experiments were performed with the pSuper plasmid (Brummelkamp et al., 2002) or its derivatives. The initial CENP-A target sequence used was 5'- ACAGTCGGCGGAGACAAGG-3' and was expressed from a version of pSuper in which we had sub-cloned the hygromycin B expression cassette from pBig2i (Strathdee et al., 1999). Following transfection of the RNAi plasmid using Effectene (Qiagen, Valencia, CA), colonies were selected using hygromycin B (Invitrogen, Carlsbad, CA; 250 μg/ml). For isolation of stable monoclonal lines, selection was allowed to continue for thirteen days so that large colonies would form that could be transferred to a well of a 96-well dish. These lines were expanded and maintained in the continued presence of hygromycin B. For the colony outgrowth assays, cells were fixed with methanol for 30 min and then stained with crystal violet. Two additional CENP-A-directed RNAi plasmids were generated in pSuper-Retro-Puro (OligoEngine, Seattle, WA) using the target sequences 5'- CCGCCTGGCAAGAGAAATA-3' and 5'-TTACATGCAGGCCGAGTTA-3', respectively, and were used in the sequential knockdown of endogenous CENP-A expression. The target sequence for YFP was 5'-GAACGGCATCAAGGTGAAC-3' which was expressed from pSuper. Co-transfection of the YFP-directed RNAi plasmid and pBABE-PURO (Morgenstern and Land, 1990) at a 10:1 ratio was followed by puromycin (Calbiochem, San Diego, CA; 1 μg/ml) selection for twelve days and crystal violet staining.

Yeast strains and constructs

All yeast strains used in this study are in S288c background. Genomic coordinates 345680 to 346408 of chromosome XI encompassing the complete *CSE4* ORF were

removed by one step gene replacement with a *TRP1* cassette in diploids resulting in strain DWCY67. Replacement was verified by PCR and by the production of 50% inviable spores upon sporulation. The complete intronless genomic *CSE4* ORF was cloned by PCR during which EcoRI and XhoI sites were added directly upsteam of the start codon and downstream of the stop codon, respectively, and the product was cloned into corresponding sites of pRS416MET25 and transformed into DWCY67. Upon sporulation, TRP+ URA+ haploids were selected creating DWCY69.

All CSE4, H3 and CSE4/H3 hybrids were constructed by PCR, overlap extension PCR (Horton et al., 1989) and by QuikChange Site-Directed Mutagenesis (Stratagene, La Jolla, CA). CSE4 and H3 sequences were derived from genomic *CSE4* and *HHT1* loci respectively. In all cases, BamHI and XhoI sites were added directly upstream and downstream of start and stop codons, respectively, and cloned into corresponding sites in pESC-HIS (Stratagene, La Jolla, CA). For construct #193, a start codon was placed in front of the lysine residue at position 130 of Cse4. For constructs #198, 200, 215, 216, and 217 amino acids 1-38 of H3 were replaced with amino acid 1-129 of Cse4 thereby replacing the H3 N-terminal tail with the Cse4 N-terminal domain (the full length H3 N-terminal tail is maintained in construct #196). The following H3→Cse4 mutations were made in constructs # 196, 200, 215, 216, and 217: K126Q and extreme C-terminal ERS(134-136)→QFI (analogous to previously identified allele *cse4-369* (Keith et al., 1999). For constructs #196, 198, 200, and 215, the region from A76 through I113 of H3 was replaced by the corresponding region containing the Loop 1 and α2 helix of Cse4 (T166 through L206). For construct #216, the region from A76 through F85 of H3 was replaced by the corresponding region of Cse4 (T166 through W178). For construct #217, the region S88 through I113 of H3 was replaced by the corresponding α2 helix of Cse4 (M181 through L206).

For construct #215, the complete ORF of yeast codon optimized GFP (derived from pFA6a-GFPMT-HIS3MX6; (Wach et al., 1997) was inserted between the last

residue of the Cse4 non-histone domain and the first residue of the H3 core domain spaced on either side with two glycine residues. All final constructs were verified by DNA sequencing.

Plasmid shuffling

DWCY69 was transformed with CSE4/H3 hybrid constructs and plated on complete synthetic dropout galactose medium lacking tryptophan and histidine but containing uracil (GALCSM-HT) to allow loss of pRS416MET25-CSE4. Colonies were scored for growth rate and replated on the same medium but 5FOA (Zymo Research) was included to select for cells that have lost pRS416MET25-CSE4. Colonies surviving 5FOA treatment were resuspended in water diluted to 10^7 cells/ml. 5 μl of 3-fold serial dilutions were spotted on GALCSM-HT medium for growth assays. In stable replacement strains, loss of wild type *CSE4* sequences and identity of the rescue construct were verified by PCR and DNA sequencing.

Chromatin IP

Cells were grown in galactose containing medium to OD_{600} 0.75, fixed in 1% formaldehyde for 10 min, and quenched with 125 mM glycine. Whole cell lysate was prepared from 75 OD units as described (Strahl-Bolsinger et al., 1997) and chromatin was sheared to an average length of ~300 base pairs by sonication. Clarified extract was used as starting material for IPs. GFP tagged proteins were immunoprecipitated using rabbit polyclonal anti-GFP antibodies immobilized on protein A support (Affi-Prep, BioRad, Hercules, CA). Precipitates were washed, de-crosslinked, and DNA was isolated as described (Strahl-Bolsinger et al., 1997). The CEN3 locus and the locus 4 kb from the centromere on the left arm were amplified using primers that have been described (Ortiz et al., 1999). A region 1.3 kb to the right of the centromere was amplified with the following oligo's: 5'-TCCCCATGTGGGAGTTCTACG and 5'-

CGAGACAGTTCCATAGCAAACTC. PCR products amplified of the 3 loci were pooled, resolved on acrylamide and stained with Ethidium Bromide.

The GFP-Cse4 control strain was constructed as follows: The 33 amino acid essential N-terminal domain (END) of Cse4 (Chen et al., 2000) and the Cse4 histone fold domain encompassing amino acid 130-229 were fused to the N- and C-terminus of yeast codon optimized GFP (from source as above) respectibely by overlap extension PCR (Horton et al., 1989). Both Cse4 domains were spaced from GFP with two glycine residues. EcoRI and BamHI sites were added by PCR directly upstream and downstream of the ORF respectively and product was cloned into pUC19. The ADH1 terminator and a URA3 cassette were inserted immediately downstream of the ORF. The entire cassette was PCR amplified to include homology arms and the product was targeted to the *CSE4* locus in diploid S288c cells replacing one *CSE4* allele (genomic coordinates 345680 to 346408 of chromosome XI, encompassing the complete *CSE4* ORF were removed) with the targeting construct which replaces the *CSE4* start codon with that from END-GFP-$CSE4_{core}$. Haploids carrying the tagged Cse4 only were isolated by sporulation and tetrads dissected. Clones were selected by uracil prototrophy and correct targeting was verified by PCR and sequencing the genomic insert.

Immunoblots

Whole cell extracts were separated by SDS-PAGE and transferred to nitrocellulose. Recombinant YFP protein (a kind gift from R. Tsien, UCSD) and CENP-A (Black et al., 2004) were used as standards to determine the level of endogenous CENP-A and exogenously expressed YFP-$H3^{CATD}$. For the immunoblots, anti-α-tubulin (DM1A, Sigma) ascites was used at a dilution of 1:4000, anti-GFP (Seedorf et al., 1999) affinity purified pAb was used at 3 μg/ml, anti-CENP-A (a kind gift from K. Yoda, Nagoya University) tissue culture supernatant was used at a dilution of 1:30, and human anti-centromere (Antibodies, Inc., Davis, CA) antibodies were used at a dilution of 1:300.

Secondary antibodies were obtained from Amersham Biosciences (Piscataway, NJ) and Jackson ImmunoResearch Laboratories (West Grove, PA).

Indirect immunofluorescence

Cells grown on glass coverslips were fixed and processed for indirect immunofluorescence. For mitotic chromosome preparations, nocodazole (Sigma, St. Louis, MO; 400 ng/ml) treated cells were harvested by agitation, hypotonically swollen in 75 mM KCl, spun onto glass slides using a Cytospin centrifuge (Thermo Electron, Waltham, MA) at 2000 rpm for 2 min, and then processed for indirect immunofluorescence. All mutations of CENP-A and $H3^{CATD}$ were generated using the Quickchange system (Stratagene, La Jolla, CA) in each respective YFP-fusion protein construct. Anti-CENP-A was used at a dilution of 1:100, anti-CENP-B (Earnshaw et al., 1987) ascites was used at a dilution of 1:200, anti-CENP-C (a kind gift from B. Earnshaw, University of Edinburgh) sera was used a dilution of 1:1000, anti-CENP-E (Brown et al., 1996) sera was used at a dilution of 1:200, anti-Mad1 (a kind gift from A. De Antoni and A. Musacchio, IEO, Milan) tissue culture supernatant was used at a dilution of 1:20, anti-Mad2 (Kops et al., 2005) affinity purified pAb was used at 1:200, and anti-aurora-B (anti-AIM1, BD Biosciences, San Jose, CA) purified mAb was used at 1.25 μg/ml. Donkey secondary antibodies (anti-mouse Cy5-conjugated, anti-rabbit Texas Red-conjugated, and anti-rabbit Cy5-conjugated) were obtained from Jackson Immunoresearch Laboratories (West Grove, PA). Samples were stained with DAPI prior to mounting with Vectashield medium (Vector Laboratories, Burlingame, CA). Digital images were captured using Deltavision Softworx software by a Roper Coolsnap interline charge-coupled device camera mounted on an Olympus IX-70 inverted microscope. For each sample, images were collected at 0.2 μm z-sections that were subsequently deconvolved using identical parameters. The z-stacks were then projected as single two-

dimensional images and assembled using Adobe Photoshop (version 7.0) and Macromedia Freehand (version 10.0).

FISH

Cells grown on coverslips were fixed in 4% formaldehyde and permeabilized with 0.1% saponin and 0.1% Triton-X 100 in PBS. After a 20 min incubation in PBS supplemented with 20% glycerol, coverslips underwent three cycles of freeze/thaw in liquid N_2, rinsed in PBS, washed twice in 2X SSC, and treated with 100 μg/ml RNase for 30 min at 37°C. Subsequently coverslips were washed twice in 2X SSC, incubated for 10 min in 0.1 M HCl, extracted again in PBS supplemented with 0.5 % saponin and 0.5% Triton-X 100, and then rinsed in PBS. Centromere specific probes for chromosome 2 and 7 were labeled with Rhodamine labeled dUTP (Roche, Indianapolis, IN). Labeled probe (5 ng/μl) and salmon sperm carrier DNA (1000 ng/μl) were resuspended in 2X SSC containing 50% formamide, 10% dextran sulfate, and 0.1% Triton-X 100. Probe mixtures were denatured just prior to hybridization for 5 min at 75°C. The coverslips containing the samples were also denatured for 5 min at 75°C in 2X SCC containing 70% formamide. Directly following the denaturation steps, coverslips were placed on 10 μl of denatured probe on a glass slide, sealed with rubber cement, and incubated for 16 h at 37°C. Coverslips were then washed once in 2X SSC containing 50% formamide for 30 min at 37 °C, twice in 2X SSC for 5 minutes at 37 °C, rinsed in PBS, stained with DAPI, and mounted with ProLong (Molecular Probes, Eugene, OR). Images were collected of 1 μm z-sections spanning the entire nucleus using a Deltavision microscope (described above). Stacks of images were subsequently deconvolved and projected as single two-dimensional images. Multiple panels were acquired allowing over 300 cells to be analyzed for each data point.

FACS analysis

Cycling cells or cells arrested for 16 h in nocodazole were harvested, fixed in ethanol (70%), washed in PBS supplemented with FBS (1%), and then stained with propidium iodide (10 μg/ml) in PBS supplemented with FBS (1%) and RNase A (250 μg/ml). DNA content was measured on a FACSVantage (BD Biosciences, San Jose, CA).

Live cell microscopy

Mitotic chromosome movements were monitored by imaging RFP-tagged histone H2B (H2B-RFP). To generate the H2B-RFP expression plasmid we first replaced the BFP open reading frame from pEBFP-N1 with RFP (version mRFP1.3 [(Shaner et al., 2004). Then we sub-cloned histone H2B (kindly provided by K. Sullivan, Scripps) into this plasmid to generate the H2B-RFP fusion protein expression cassette. In all of our live cell experiments, this plasmid was co-transfected with RNAi plasmid mixes at a ratio of 1:10. Cells were plated on glass-bottomed 35 mm dishes (MatTek, Ashland, MA) 36-48 hours prior to analysis. Just before imaging, the media was replaced with CO_2-independent media (Invitrogen, Carlsbad, CA) supplemented with 10% FBS. A layer of mineral oil covered the media to prevent evaporation. Time-lapse images were captured with a Hamamatsu Orca ER charge coupled device camera mounted on a spinning disk confocal (McBain Instruments, Chatsworth, CA) attached to a Nikon TE2000e inverted microscope equipped a 60X/NA1.4 objective lens. Media temperature was maintained at 34-37^{o}C at all times with a heated stage, and this was externally monitored using a thermocouple. Images were acquired for YFP and RFP channels, as well as differential interference contrast (DIC) at one min intervals. For each time-point, 5 X 1 μm z-sections were acquired for fluorescence images and a single DIC image was acquired at the middle z-position using Metamorph software. Images were processed for movies and stills using Metamorph. For chromosome motility measurements, at least 15

chromosomes from at least 5 cells were monitored and distance measurements were made using standard methods in Metamorph.

For yeast imaging, 5FOA resistant Y69 strain carrying construct #215 and lacking CSE4 was grown in (GALCSM-HT) to mid log phase and spotted on a 2% low melting agar slab in the same medium. The slab was sealed with a cover slip and VALAP (Vaseline : lanolin : paraffin 1:1:1 [w/w]) and imaged by spinning disk confocal microscopy with a 60X objective and 1.5X auxiliary magnification. A stack of 5 images at 1 μm intervals were acquired for fluorescence images and a single DIC image was acquired at the middle z-position. Stacks of acquisitions (1 min intervals) were projected to flattened images post-acquisition using Metamorph software.

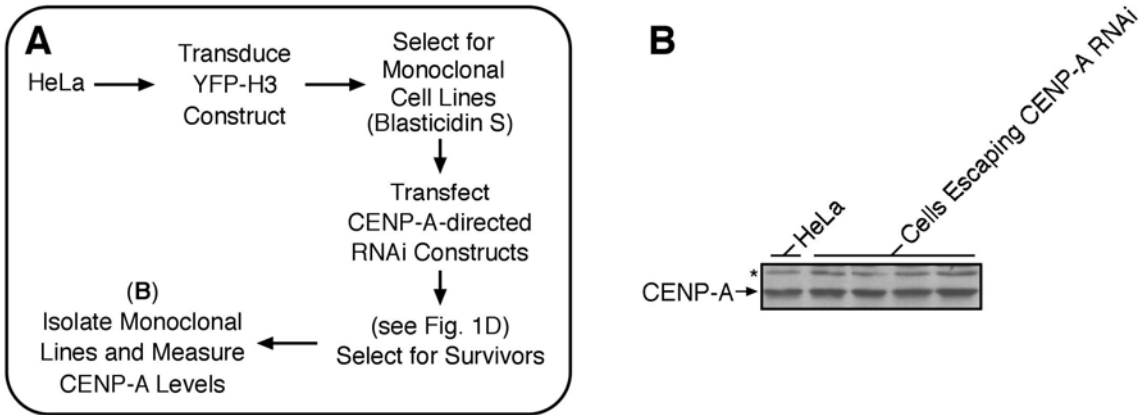

Fig. S1. Escape from CENP-A RNAi in survivors from the YFP-H3-expressing control HeLa line. (A) Experimental scheme. Despite lacking a rescue construct containing YFP-H3^{CATD}, the YFP-H3-expressing control HeLas generated a small number of surviving colonies after selection of the plasmid expressing CENP-A-directed RNAi (see scheme in Figure 1 D & E). From a colony selection plate not used for crystal violet staining, we isolated, expanded, and prepared these lines for immunoblot analysis (**B**). Here, four separate lines were analyzed for CENP-A levels and compared to control

HeLa cells. The asterisk marks the mobility of a cross-reacting band that serves as an internal loading control. There is no detectable decrease of CENP-A protein levels in these cells, indicating that the YFP-H3 control HeLas have escaped CENP-A-directed RNAi knockdown despite obtaining resistance to hygromycin.

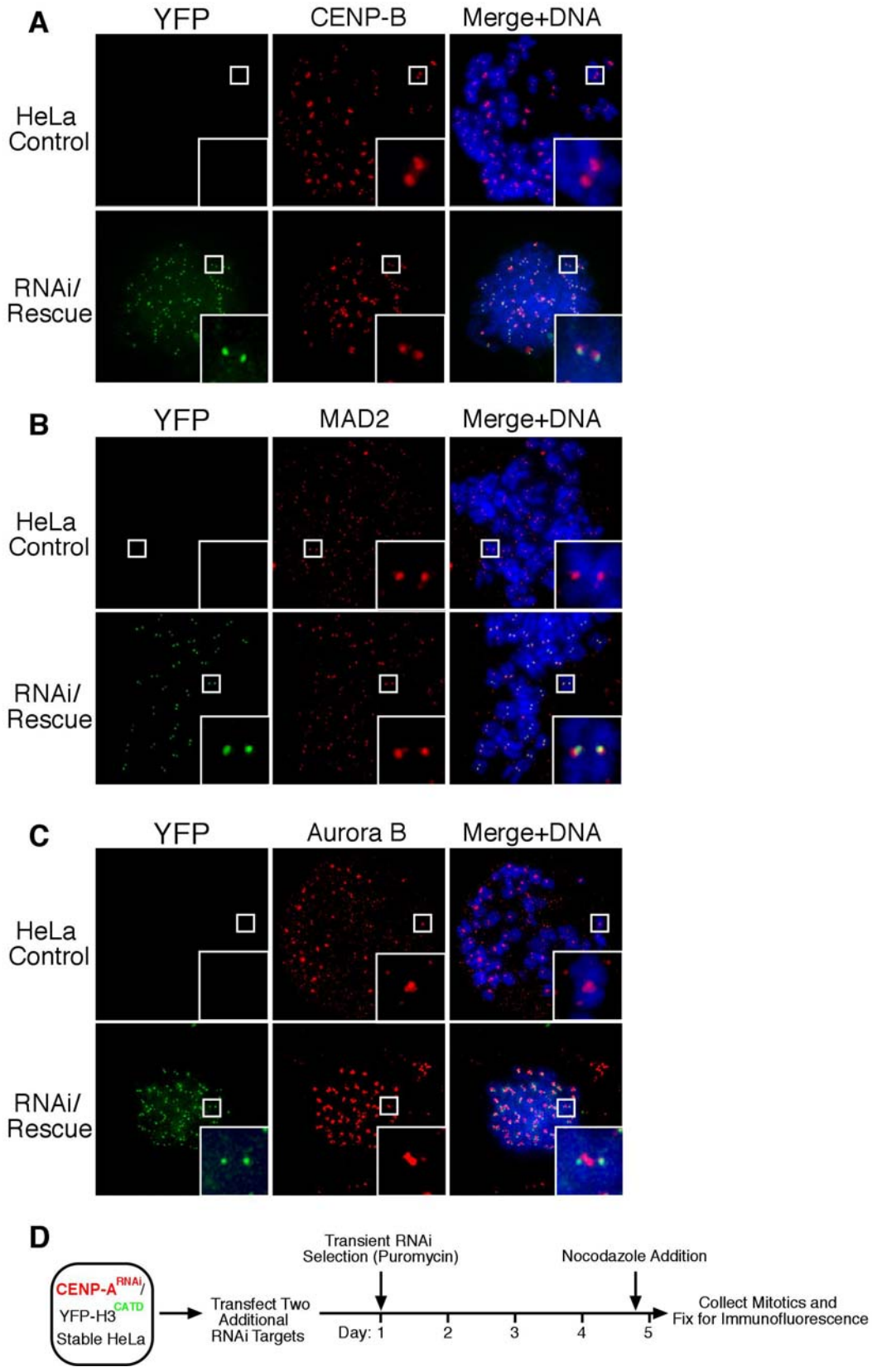
A
YFP
CENP-B
Merge+DNA
HeLa Control
RNAi/ Rescue
B
YFP
MAD2
Merge+DNA
HeLa Control
RNAi/ Rescue
C
YFP
Aurora B
Merge+DNA
HeLa Control
RNAi/ Rescue
D
CENP-A RNAi/ YFP-H3 CATD Stable HeLa
Transfect Two Additional RNAi Targets
Transient RNAi Selection (Puromycin)
Nocodazole Addition
Day: 1 2 3 4 5
Collect Mitotics and Fix for Immunofluorescence

Fig. S2. Intact kinetochores in YFP-H3^{CATD}-expressing cells upon depletion of CENP-A. CENP-B (**A**), an inner kinetochore component, Mad2 (**B**), an outer kinetochore component, and Aurora B (**C**), an inner centromere component, are each localized properly on mitotic kinetochores in RNAi/Rescue cells. (**D**) Scheme for analysis of mitotic kinetochores in CATD Rescue cells.

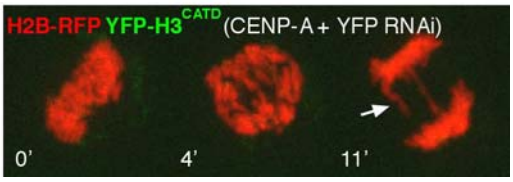

Fig. S3. Lagging chromosomes in the small proportion of cells that progress past metaphase in cells depleted for both CENP-A and the rescuing YFP-H3^{CATD}. Stills from Movie S6 showing a cell attempting to progress through mitosis despite the co-depletion of CENP-A and YFP-H3^{CATD}. In the rare instance that these cells progress past metaphase, lagging chromosomes are clearly present (the one marked with an arrow in the 11' still image) is left behind in the center as chromosomes progress poleward), indicative of centromere defects.

Black et al.
Figure S4

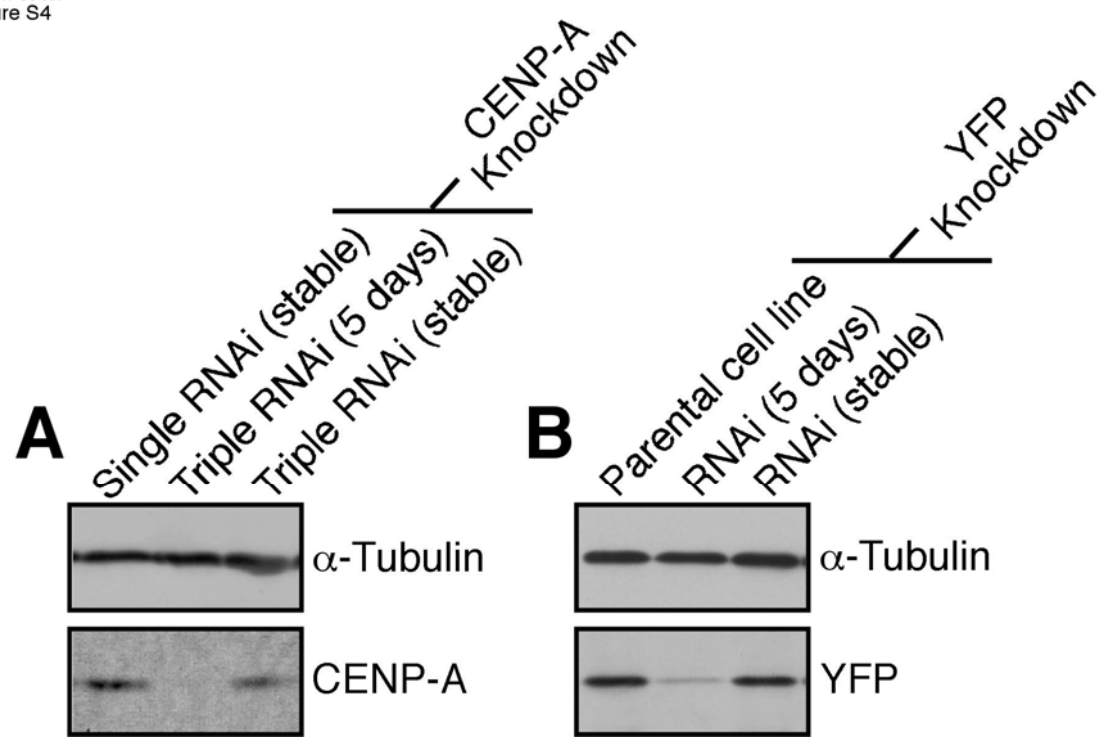

Fig. S4. Robust knockdown of endogenous CENP-A after 5 days of sequential and selectable plasmid-based RNAi (**A**) Knockdown after transient triple knockdown and re-emergence of endogenous CENP-A after selection of stable puromycin resistant cells. (**B**) Re-emergence of YFP-expression in a parental cell line expressing YFP-H3^{CATD} on top of normal levels of CENP-A. This shows that the re-emergence is a property of the RNAi cassette selection for stable expression.

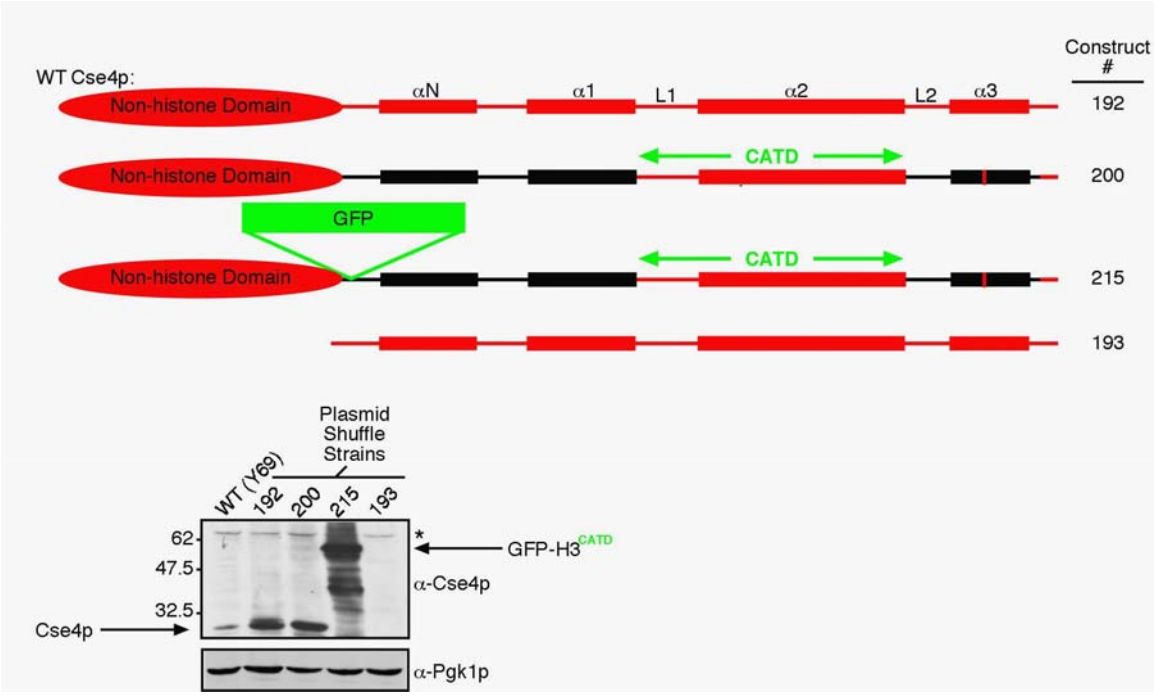

Fig. S5. Immunoblot of *cse4Δ* rescue constructs. Extracts from 1 X 10^7 yeast cells were separated by SDS-PAGE for strains where *CSE4* is replaced by the indicated constructs after galactose-induced expression. Immunoblotting was performed using a rabbit polyclonal antibody raised against and affinity purified with a recombinant version of the N-terminus of Cse4p (amino acids 93-140). The asterisk marks a yeast protein that is non-specifically recognized by this antibody. Endogenous Cse4p is recognized in the WT (Y69) strain at ~27 kDa. The bands between ~40 and 50 kDa and below the major band (~55 kDa) for construct #215 appear to be degradation products. Construct #193 does not contain the N-terminal antigenic sequence, and the protein it encodes is not recognized by this antibody. The blot was also probed for Pgk1p using a mAb from Molecular Probes, as a loading control.

Supplemental References

Black, B. E., Foltz, D. R., Chakravarthy, S., Luger, K., Woods, V. L., and Cleveland, D. W. (2004). Structural determinants for generating centromeric chromatin. Nature *430*, 578-582.

Brown, K. D., Wood, K. W., and Cleveland, D. W. (1996). The kinesin-like protein CENP-E is kinetochore-associated throughout poleward chromosome segregation during anaphase-A. J Cell Sci *109 (Pt 5)*, 961-969.

Brummelkamp, T. R., Bernards, R., and Agami, R. (2002). A system for stable expression of short interfering RNAs in mammalian cells. Science *296*, 550-553.

Chen, Y., Baker, R. E., Keith, K. C., Harris, K., Stoler, S., and Fitzgerald-Hayes, M. (2000). The N terminus of the centromere H3-like protein Cse4p performs an essential function distinct from that of the histone fold domain. Mol Cell Biol *20*, 7037-7048.

Earnshaw, W. C., Sullivan, K. F., Machlin, P. S., Cooke, C. A., Kaiser, D. A., Pollard, T. D., Rothfield, N. F., and Cleveland, D. W. (1987). Molecular cloning of cDNA for CENP-B, the major human centromere autoantigen. J Cell Biol *104*, 817-829.

Horton, R. M., Hunt, H. D., Ho, S. N., Pullen, J. K., and Pease, L. R. (1989). Engineering hybrid genes without the use of restriction enzymes: gene splicing by overlap extension. Gene *77*, 61-68.

Keith, K. C., Baker, R. E., Chen, Y., Harris, K., Stoler, S., and Fitzgerald-Hayes, M. (1999). Analysis of primary structural determinants that distinguish the centromere-specific function of histone variant Cse4p from histone H3. Mol Cell Biol *19*, 6130-6139.

Kops, G. J., Kim, Y., Weaver, B. A., Mao, Y., McLeod, I., Yates, J. R., 3rd, Tagaya, M., and Cleveland, D. W. (2005). ZW10 links mitotic checkpoint signaling to the structural kinetochore. J Cell Biol *169*, 49-60.

Morgenstern, J. P., and Land, H. (1990). Advanced mammalian gene transfer: high titre retroviral vectors with multiple drug selection markers and a complementary helper-free packaging cell line. Nucleic Acids Res *18*, 3587-3596.

Ortiz, J., Stemmann, O., Rank, S., and Lechner, J. (1999). A putative protein complex consisting of Ctf19, Mcm21, and Okp1 represents a missing link in the budding yeast kinetochore. Genes Dev *13*, 1140-1155.

Seedorf, M., Damelin, M., Kahana, J., Taura, T., and Silver, P. A. (1999). Interactions between a nuclear transporter and a subset of nuclear pore complex proteins depend on Ran GTPase. Mol Cell Biol *19*, 1547-1557.

Shah, J. V., Botvinick, E., Bonday, Z., Furnari, F., Berns, M., and Cleveland, D. W. (2004). Dynamics of centromere and kinetochore proteins; implications for checkpoint signaling and silencing. Curr Biol *14*, 942-952.

Shaner, N. C., Campbell, R. E., Steinbach, P. A., Giepmans, B. N., Palmer, A. E., and Tsien, R. Y. (2004). Improved monomeric red, orange and yellow fluorescent proteins derived from Discosoma sp. red fluorescent protein. Nat Biotechnol *22*, 1567-1572.

Strahl-Bolsinger, S., Hecht, A., Luo, K., and Grunstein, M. (1997). SIR2 and SIR4 interactions differ in core and extended telomeric heterochromatin in yeast. Genes Dev *11*, 83-93.

Strathdee, C. A., McLeod, M. R., and Hall, J. R. (1999). Efficient control of tetracycline-responsive gene expression from an autoregulated bi-directional expression vector. Gene *229*, 21-29.

Wach, A., Brachat, A., Alberti-Segui, C., Rebischung, C., and Philippsen, P. (1997). Heterologous HIS3 marker and GFP reporter modules for PCR-targeting in Saccharomyces cerevisiae. Yeast *13*, 1065-1075.